NASA Technical Memorandum 78650

Wind-Tunnel Results for an Improved 21-Percent-Thick Low-Speed Airfoil Section

Robert J. McGhee and William D. Beasley

APRIL 1978

NASA

NASA Technical Memorandum 78650

Wind-Tunnel Results for an Improved 21-Percent-Thick Low-Speed Airfoil Section

Robert J. McGhee and William D. Beasley
Langley Research Center
Hampton, Virginia

SUMMARY

An investigation was conducted in the Langley low-turbulence pressure tunnel to evaluate the effects on performance of modifying a 21-percent-thick low-speed airfoil. The airfoil contour was altered to reduce the upper-surface adverse pressure gradient and hence reduce boundary-layer separation. The tests were conducted at free-stream Mach numbers from 0.10 to 0.28. The chord Reynolds number varied from about 2.0×10^6 to 9.0×10^6.

The results indicate that the modification to the airfoil contour increased the value of the maximum lift-drag ratio of the airfoil at all test Reynolds numbers. For example, at a Reynolds number of 4.0×10^6, changing the airfoil contour increased the maximum lift-drag ratio from about 60 to 85. This improvement in performance is attributed to reduced upper-surface boundary-layer separation for the modified airfoil. Also, the results show that the modification to the airfoil decreased the magnitude of the quarter-chord pitching-moment coefficient at the design lift coefficient. The largest value of maximum lift coefficient for the modified airfoil with roughness located near the leading edge was about 1.80 in comparison with about 1.70 for the original airfoil.

INTRODUCTION

Research on an initial thickness family of airfoils developed for low-speed general aviation application is reported in reference 1. Results of this research showed that the 21-percent-thick airfoil of this family provided a substantial improvement in maximum lift coefficient in comparison with the older 21-percent-thick NACA airfoils. However, this thick airfoil displayed poor aerodynamic efficiency (lift-drag ratio) in comparison with the thinner airfoils of the thickness family because of extensive turbulent boundary-layer thickening and separation at low Reynolds numbers. Therefore, this airfoil (LS(1)-0421) has been analytically reshaped in order to decrease substantially the upper-surface adverse pressure gradient in an attempt to reduce the amount of separation on the airfoil. This report presents the basic low-speed section characteristics of this modified airfoil and evaluates the effects on performance resulting from the change in airfoil shape.

The investigation was performed in the Langley low-turbulence pressure tunnel at free-stream Mach numbers from 0.10 to 0.28. The chord Reynolds number varied from about 2.0×10^6 to 9.0×10^6, and the geometrical angle of attack varied from about -8° to 20°.

SYMBOLS

Values are given in both SI and U.S. Customary Units. The measurements and calculations were made in U.S. Customary Units.

C_p pressure coefficient, $\dfrac{p_l - p_\infty}{q_\infty}$

c   airfoil chord, centimeters (inches)

c_c section chord-force coefficient, $\displaystyle\int \tilde{C}_p \, d\!\left(\dfrac{z}{c}\right)$

c_d section profile-drag coefficient, $\displaystyle\int_{wake} c_d{}' \, d\!\left(\dfrac{h}{c}\right)$

$c_d{}'$ point-drag coefficient (ref. 6)

c_l section lift coefficient, $c_n \cos \alpha - c_c \sin \alpha$

c_m section pitching-moment coefficient about quarter-chord point,

$$-\int C_p \left(\dfrac{x}{c} - 0.25\right) d\!\left(\dfrac{x}{c}\right) + \int C_p \left(\dfrac{z}{c}\right) d\!\left(\dfrac{z}{c}\right)$$

c_n section normal-force coefficient, $\displaystyle -\int C_p \, d\!\left(\dfrac{x}{c}\right)$

h   vertical distance in wake profile, centimeters (inches)

l/d section lift-drag ratio, c_l/c_d

M   free-stream Mach number

p   static pressure, N/m^2 (lb/ft^2)

q   dynamic pressure, N/m^2 (lb/ft^2)

R   Reynolds number based on free-stream conditions and airfoil chord

S   separation point

t   airfoil thickness, centimeters (inches)

x   airfoil abscissa, centimeters (inches)

z   airfoil ordinate, centimeters (inches)

z_c mean camber line ordinate, centimeters (inches)

z_t mean thickness, centimeters (inches)

2

α geometric angle of attack, degrees

Subscripts:

l local point on airfoil

max   maximum

∞ free-stream condition

Abbreviations:

LS(1)   low-speed first series

Mod   modified

AIRFOIL MODIFICATION

The airfoil contour was changed to reduce the magnitude of the adverse upper-surface pressure gradient and hence to decrease boundary-layer separation. The maximum thickness ratio, trailing-edge thickness, and design lift coefficient ($c_l = 0.40$) of the original airfoil were retained.

The modification to the surface contour of airfoil LS(1)-0421 is illustrated in figure 1. The upper-surface modification was accomplished by adding material from approximately the 0.5-percent-chord station, fairing with the original airfoil at about the 35-percent-chord station, and removing material from this station to the airfoil trailing edge. The lower-surface modification was accomplished by adding a small amount of material from the station at approximately 70-percent chord to the airfoil trailing edge. The maximum thickness of the modified airfoil was moved forward from the 40-percent-chord station to the station at 32.5-percent chord. Figure 2 compares the mean thickness and camber distributions for the two airfoils, and figure 3 compares the surface slope distributions. Coordinates for both airfoils are presented in tables I and II.

The results of reference 1 showed that experimental section data and the theoretical viscous method of reference 2 agreed well for attached boundary layers for airfoils of thickness ratios of 13 and 17 percent, but agreement was poor for the 21-percent airfoil. Figure 4, which was prepared prior to the modification, shows the comparison between experiment and two different viscous theories for the LS(1)-0421 airfoil for a Reynolds number of 4.0×10^6. The theoretical analysis code of reference 3 agrees reasonably well with the experimental lift data and indicates a conservative estimate of boundary-layer separation. Therefore, the analysis program of reference 3 was used in modifying the 21-percent-thick airfoil.

Theoretical pressure distributions for both airfoils are shown in figure 5 for a Reynolds number of 4.0×10^6. Boundary-layer transition was specified at $x/c = 0.03$ for the calculations to ensure a turbulent boundary-layer development on the airfoils. At a lift coefficient of 0.40 (fig. 5(a)), the theory

3

indicates a decrease in the extent of upper-surface separation of about 0.05c
for the modified airfoil; however, at a lift coefficient of 1.0 (fig. 5(b)) a
decrease of about 0.10c is shown. Based on these theoretical results the
desired decrease in separation would be expected for the modified airfoil.
The maximum lift coefficients for the airfoils could not be determined from
the theory because the present methods cannot properly treat the flow field
where extensive regions of separation are present.

MODELS, APPARATUS, AND PROCEDURE

Models

The airfoil models were constructed with a metal core around which plastic
fill and two thin layers of fiberglass formed the contour of the airfoils. The
models had chords of 61 cm (24 in.) and spans of 91 cm (36 in.). The models
were equipped with both upper- and lower-surface orifices located 5 cm (2 in.)
off the midspan. The airfoil surface was sanded in the chordwise direction with
No. 400 dry silicon carbide paper to provide a smooth aerodynamic finish. The
model contour accuracy was generally within ±0.10 mm (0.004 in.).

Wind Tunnel

The Langley low-turbulence pressure tunnel (ref. 4) is a closed-throat,
single-return tunnel which can be operated at stagnation pressures from 1 to
10 atmospheres (1 atm = 101.3 kPa) with tunnel-empty test-section Mach numbers
up to 0.42 and 0.22, respectively. The maximum unit Reynolds number is about
49×10^6 per m (15×10^6 per ft) at a free-stream Mach number of about 0.22.
The tunnel test section is 91 cm (3 ft) wide by 229 cm (7.5 ft) high.

Hydraulically actuated circular plates provided positioning and attach-
ment for the two-dimensional model. The plates are 102 cm (40 in.) in diameter,
rotate with the airfoil, and are flush with the tunnel wall. The airfoil ends
were attached to rectangular model attachment plates (fig. 6), and the airfoil
was mounted so that the center of rotation of the circular plates was at 0.25c
on the model reference line. The air gaps at the tunnel walls between the rec-
tangular plates and the circular plates were sealed with flexible sliding metal
seals. (See fig. 6.)

Wake Survey Rake

A fixed wake survey rake (fig. 7) at the model midspan was cantilever
mounted from the tunnel sidewall and located one chord length behind the trail-
ing edge of the airfoil. The wake rake had total-pressure tubes, 0.15 cm
(0.060 in.) in diameter, and static-pressure tubes, 0.32 cm (0.125 in.) in
diameter. The total-pressure tubes were flattened to 0.10 cm (0.040 in.) for
0.61 cm (0.24 in.) from the tip of the tube. Each static-pressure tube had
four flush orifices drilled 90° apart; the orifices were located 8 tube diam-
eters from the tip of the tube in the measurement plane of the total-pressure
tubes.

Instrumentation

The static pressures on the airfoil surfaces and the wake rake pressures were measured by an automatic pressure-scanning system using variable-capacitance precision transducers. Basic tunnel pressures were measured with precision quartz manometers. Angle of attack was measured with a calibrated digital shaft encoder operated by a pinion gear and rack attached to the circular model attachment plates. Data were obtained by a high-speed acquisition system and were recorded on magnetic tape.

TESTS AND METHODS

The modified airfoil was tested at free-stream Mach numbers from 0.10 to 0.28 over an angle-of-attack range from about -8° to 20°. The Reynolds number based on the airfoil chord was varied from about 2.0×10^6 to 9.0×10^6. The airfoil was tested both smooth (natural transition) and with roughness located on both upper and lower surfaces at 0.075c. The roughness was sized for each Reynolds number according to the technique in reference 5. The roughness was sparsely distributed and consisted of granular-type strips 0.13 cm (0.05 in.) wide which were attached to the surfaces with clear lacquer.

The static-pressure measurements at the airfoil surface were reduced to standard pressure coefficients and were machine integrated to obtain section normal-force and chord-force coefficients and section pitching-moment coefficients about the quarter-chord point. Section profile-drag coefficient was computed from the wake rake total and static pressures by the method reported in reference 6.

An estimate of the standard low-speed wind-tunnel boundary corrections (ref. 7) amounted to a maximum of about 2 percent of the measured coefficients; these corrections have not been applied to the data.

PRESENTATION OF RESULTS

The results of this investigation have been reduced to coefficient form and are presented in the following figures:

DISCUSSION OF RESULTS

Pressure Distributions

The airfoil contour modification at the design condition produced the desired decrease in the upper-surface adverse pressure gradient shown by the experimental pressure data comparison for both airfoils in figure 12. Altering the shape of the !S(1)-0421 airfoil resulted in an increase in upper-surface curvature in the forward region of the airfoil and a decrease in curvature in the aft region. Figure 12(a) for $\alpha \approx 0°$ illustrates the change in pressure distribution resulting from these surface curvature changes. Note that the change in airfoil contour moved the start of the upper-surface pressure recovery forward about 0.30c. Figures 12(b) and 12(c) compare the pressure data for both airfoils for angles of attack of about 4° and 8° for a Reynolds number of 4.0×10^6. At $\alpha \approx 4°$ the aft upper-surface pressure recovery for the LS(1)-0421 airfoil is typical of that for thick turbulent boundary layers approaching separation. At $\alpha \approx 8°$ separation is indicated by the lack of pressure gradient on the aft upper surface of the airfoil. A reduction in the extent of separation of about 0.20c is shown for the modified airfoil for $\alpha \approx 8°$. Figure 12(d) compares the pressure data for the two airfoils at $\alpha \approx 14°$. For this angle of attack the LS(1)-0421 airfoil is near maximum lift and the modified airfoil is beyond its stall angle. (See fig. 10(b).) The earlier stall for the modified airfoil is attributed to the absence of the reduced pressure gradient near the airfoil midchord. (See fig. 12(b).) This reduced pressure gradient retards the rapid forward movement of upper-surface separation at the onset of stall.

Small effects only of changing Reynolds number on the pressure distribution of either airfoil at $\alpha = 0°$ are indicated by the comparison of figure 12(a) $(R = 4.0 \times 10^6)$ with figure 12(e) $(R = 9.0 \times 10^6)$. The section data for the LS(1)-0421 airfoil (fig. 10) show a decrease in lift coefficient of about 0.06 at $\alpha = 0°$ as the Reynolds number is decreased from 9.0×10^6 to 4.0×10^6, but the modified airfoil shows only a small change. This decrease in lift coefficient for the original airfoil results from an increase in boundary-layer displacement thickness at the lower Reynolds number; this increase decambers the airfoil. A comparison of figures 12(b) $(R = 4.0 \times 10^6)$ and 12(f) $(R = 9.0 \times 10^6)$ for $\alpha = 4°$ shows a decrease in upper-surface trailing-edge separation of about 0.05c for the LS(1)-0421 airfoil as the Reynolds number is increased from 4.0×10^6 to 9.0×10^6.

Section Characteristics

The section characteristics for both airfoils are compared in figure 10 for Reynolds numbers from 2.0×10^6 to 9.0×10^6. For the test Reynolds number

6

range, the modified airfoil displays a higher lift-curve slope, a more linear lift curve, and an improvement in maximum lift-drag ratio (fig. 14). This result is attributed to reduced upper-surface separation for the modified airfoil. For a Reynolds number of 4.0×10^6 (fig. 14) $(1/d)_{max}$ is increased from 60 to 85 for the modified airfoil. This value of $(1/d)_{max}$ for the modified airfoil compares favorably with the value for the 17-percent-thick airfoil of this family (ref. 1). Figure 14 also indicates that the lift coefficient for $(1/d)_{max}$ has been increased for the modified airfoil.

The stall characteristics for both airfoils are of the trailing-edge type as shown by figures 10 and 12(d). The nature of the stall for the modified airfoil at a Reynolds number of 2.0×10^6 (fig. 10(a)) is interesting because $c_{l_{max}}$ is reached at $\alpha = 12^o$ and remains relatively constant at poststall

angles of attack. Increasing the Reynolds number results in a more abrupt stall for the modified airfoil. Figure 13 compares the values of $c_{l_{max}}$ for both

airfoils, with and without roughness, for a Reynolds number range from 2.0×10^6 to 9.0×10^6. In the smooth condition the original airfoil shows higher values of $c_{l_{max}}$ at both the lowest and highest Reynolds numbers. The erratic vari-

ation of $c_{l_{max}}$ with Reynolds number exists with or without roughness for the

original airfoil but has been removed for the modified airfoil. Also, at the higher Reynolds numbers the sensitivity of $c_{l_{max}}$ to roughness has been

decreased for the redesigned airfoil. The largest value of $c_{l_{max}}$ with rough-

ness on was about 1.8 for the modified airfoil compared to about 1.7 for the original airfoil.

Figure 9 indicates that for free-stream Mach numbers from 0.10 to 0.28 the modified airfoil exhibits only small effects on the section characteristics. This result was also reported (ref. 1) for the original airfoil. Figure 10 shows a decrease in the magnitude of the quarter-chord pitching-moment coefficients for the modified airfoil compared to the original airfoil at the design lift coefficient ($c_l = 0.40$). This result is associated with the reduction in aft camber and the increase in forward loading for the modified airfoil and is indicated by the comparison of camber distributions in figure 2.

CONCLUDING REMARKS

Low-speed wind-tunnel tests have been conducted in the Langley low-turbulence pressure tunnel to evaluate the effects on performance of modifying a 21-percent-thick airfoil. The airfoil contour was altered to reduce the upper-surface adverse pressure gradient and hence reduce boundary-layer separation. The tests were conducted at free-stream Mach numbers from 0.10 to 0.28. The chord Reynolds number varied from about 2.0×10^6 to 9.0×10^6.

The results show that the modification to the airfoil contour increased the value of the maximum lift-drag ratio of the airfoil at all test Reynolds

7

numbers. For example, at a Reynolds number of 4.0×10^6, changing the air-
foil contour increased the maximum lift-drag ratio from about 60 to 85. This
improvement in performance is attributed to reduced upper-surface boundary-
layer separation for the modified airfoil. Also, the results show that the
modification to the airfoil decreased the magnitude of the quarter-chord
pitching-moment coefficient at the design lift coefficient. The largest value
of maximum lift coefficient for the modified airfoil with roughness located
near the leading edge was about 1.80 in comparison with about 1.70 for the
original airfoil.

Langley Research Center
National Aeronautics and Space Administration
Hampton, VA 23665
February 17, 1978

REFERENCES

1. McGhee, Robert J.; and Beasley, William D.: Effects of Thickness on the
   Aerodynamic Characteristics of an Initial Low-Speed Family of Airfoils
   for General Aviation Applications. NASA TM X-72843, 1976.

2. Smetana, Frederick, O.; Summey, Delbert C.; Smith, Neill S.; and Carden,
   Ronald K.: Light Aircraft Lift, Drag, and Moment Prediction - A Review
   and Analysis. NASA CR-2523, 1975.

3. Bauer, Frances; Garabedian, Paul; Korn, David; and Jameson, Antony:
   Supercritical Wing Sections II. Volume 108 of Lecture Notes in Economics
   and Mathematical Systems, Springer-Verlag, 1975.

4. Von Doenhoff, Albert E.; and Abbott, Frank T., Jr.: The Langley Two-
   Dimensional Low-Turbulence Pressure Tunnel. NACA TN 1283, 1947.

5. Braslow, Albert L; and Knox, Eugene C.: Simplified Method for Determination
   of Critical Height of Distributed Roughness Particles for Boundary-Layer
   Transition at Mach Numbers From 0 to 5. NACA TN 4363, 1958.

6. Pankhurst, R. C.; and Holder, D. W.: Wind-Tunnel Technique. Sir Isaac
   Pitman and Sons, Ltd. (London), 1965.

7. Pope, Alan; and Harper, John J.: Low-Speed Wind Tunnel Testing. John
   Wiley & Sons, Inc., c.1966.

8

TABLE I.- LS(1)-0421 AIRFOIL COORDINATES

x/c	$(z/c)_{upper}$	$(z/c)_{lower}$
0.00000	0.00000	0.00000
.00200	.01560	-.01070
.00500	.02380	-.01770
.01250	.03600	-.02650
.02500	.04910	-.03520
.03750	.05850	-.04140
.05000	.06610	-.04650
.07500	.07770	-.05460
.10000	.08660	-.06100
.12500	.09390	-.06610
.15000	.09990	-.07040
.17500	.10510	-.07390
.20000	.10940	-.07690
.22500	.11320	-.07940
.25000	.11620	-.08130
.27500	.11860	-.08260
.30000	.12070	-.08380
.32500	.12240	-.08440
.35000	.12340	-.08480
.37500	.12410	-.08470
.40000	.12440	-.08450
.42500	.12420	-.08380
.45000	.12360	-.08290
.47500	.12270	-.08150
.50000	.12110	-.07970
.52500	.11910	-.07730
.55000	.11660	-.07450
.57500	.11340	-.07100
.60000	.10970	-.06700
.62500	.10530	-.06250
.65000	.10030	-.05750
.67500	.09470	-.05230
.70000	.08860	-.04680
.72500	.08220	-.04120
.75000	.07530	-.03550
.77500	.06810	-.03000
.80000	.06070	-.02460
.82500	.05320	-.01950
.85000	.04550	-.01500
.87500	.03770	-.01110
.90000	.03000	-.00810
.92500	.02230	-.00600
.95000	.01480	-.00520
.97500	.00730	-.00590
1.00000	.00020	-.00890

TABLE II.- LS(1)-0421 MOD AIRFOIL COORDINATES

x/c	$(z/c)_{upper}$	$(z/c)_{lower}$
0.00000	0.00000	0.00000
.00200	.01560	-.01070
.00500	.02430	-.01770
.01250	.03830	-.02650
.02500	.05400	-.03520
.03750	.06510	-.04160
.05000	.07360	-.04680
.07500	.08650	-.05500
.10000	.09600	-.06140
.12500	.10340	-.06650
.15000	.10930	-.07070
.17500	.11410	-.07410
.20000	.11790	-.07700
.22500	.12080	-.07940
.25000	.12290	-.08130
.27500	.12430	-.08280
.30000	.12500	-.08390
.32500	.12500	-.08460
.35000	.12440	-.08490
.37500	.12330	-.08490
.40000	.12170	-.08460
.42500	.11960	-.08390
.45000	.11700	-.08280
.47500	.11400	-.08130
.50000	.11060	-.07940
.52500	.10680	-.07700
.55000	.10270	-.07400
.57500	.09830	-.07050
.60000	.09360	-.06660
.62500	.08860	-.06230
.65000	.08330	-.05760
.67500	.07780	-.05250
.70000	.07210	-.04720
.72500	.06620	-.04180
.75000	.06010	-.03640
.77500	.05390	-.03100
.80000	.04760	-.02560
.82500	.04120	-.02060
.85000	.03480	-.01590
.87500	.02840	-.01180
.90000	.02200	-.00860
.92500	.01560	-.00700
.95000	.00910	-.00690
.97500	.00250	-.00880
1.00000	-.00420	-.01320
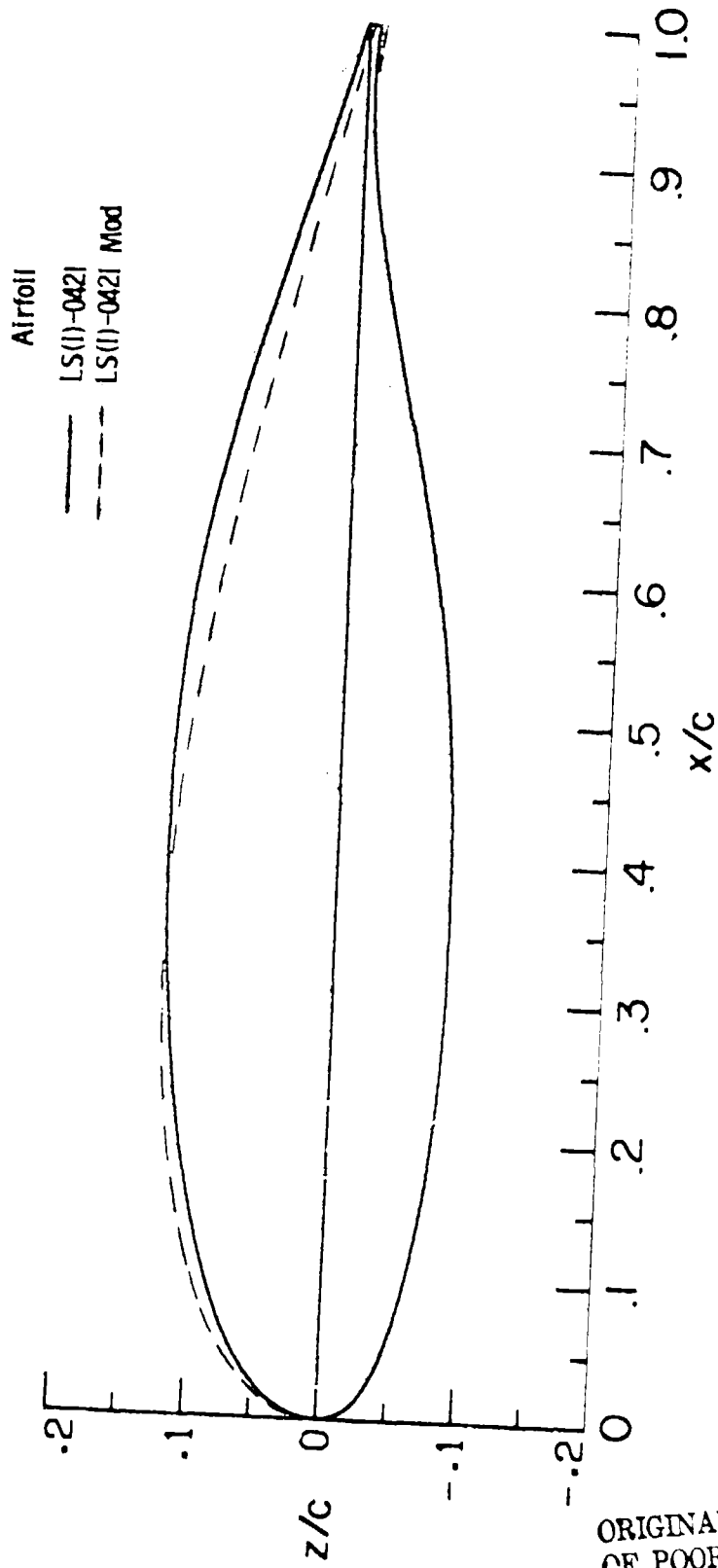
Figure 1.- Comparison of section shapes for LS(1)-0421 and LS(1)-0421 modified airfoils.

11
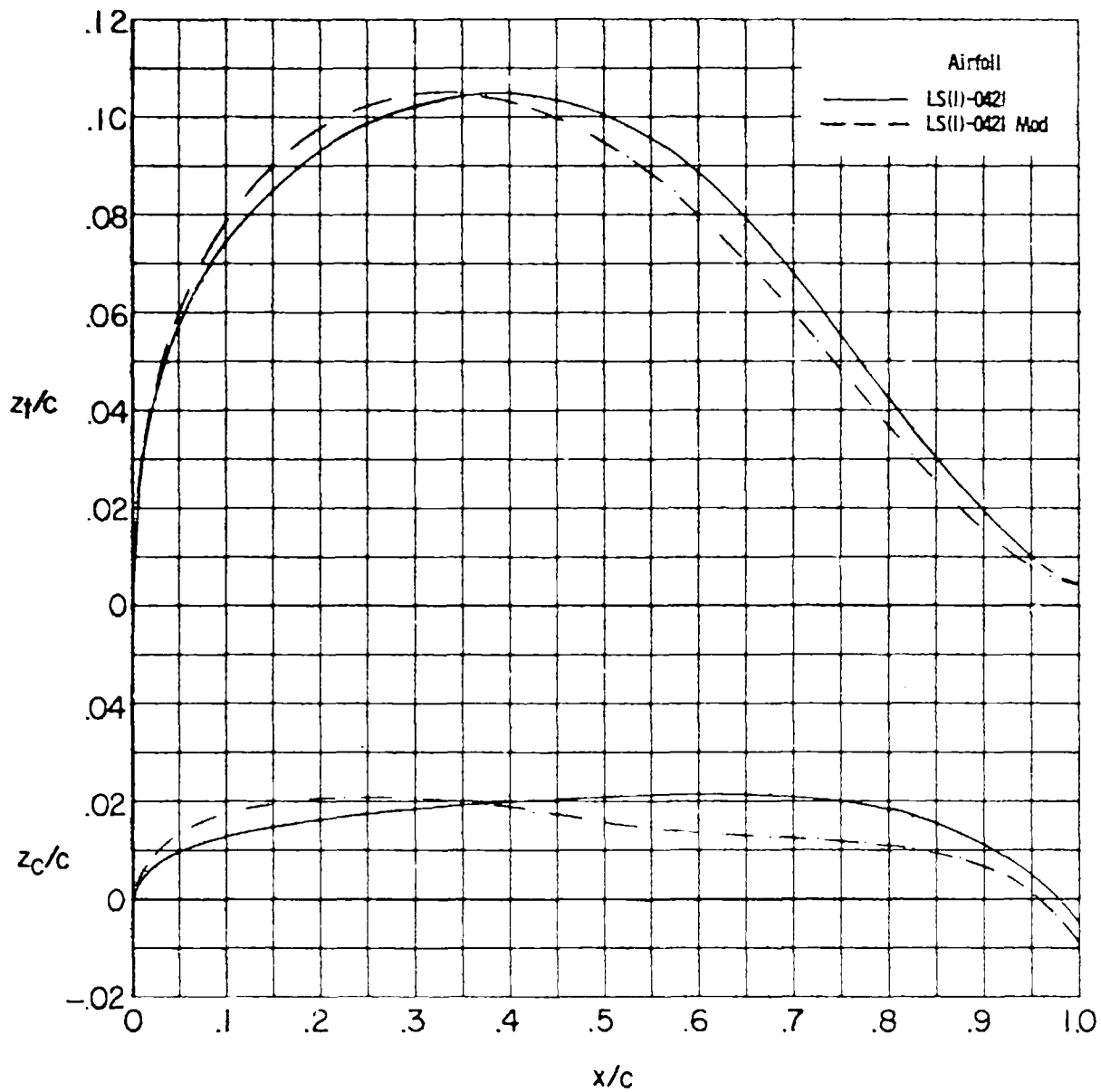
Figure 2.- Comparison of mean thickness distributions and camber lines for LS(1)-0421 and LS(1)-0421 modified airfoils.
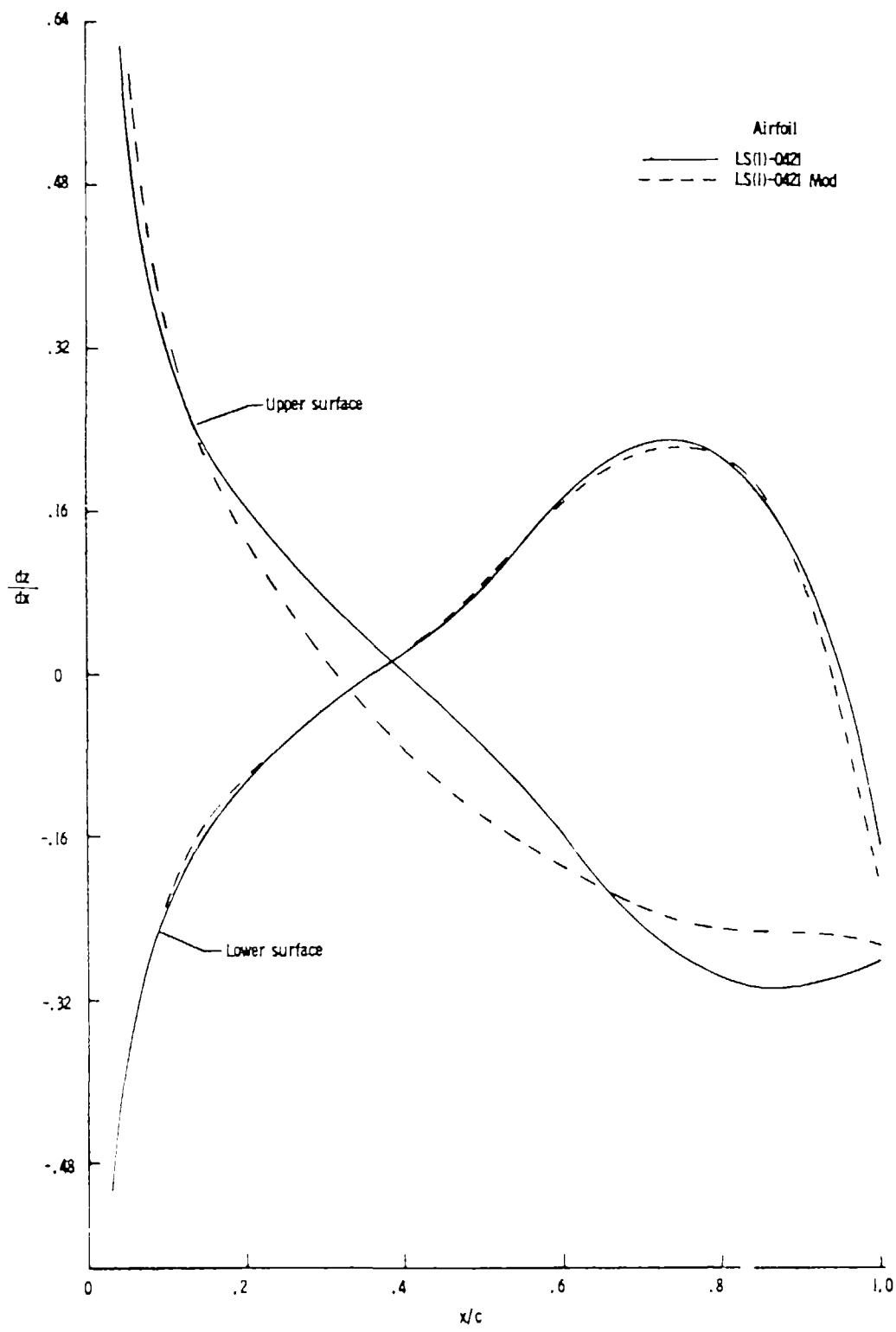
Figure 3.- Chordwise distribution of slopes.
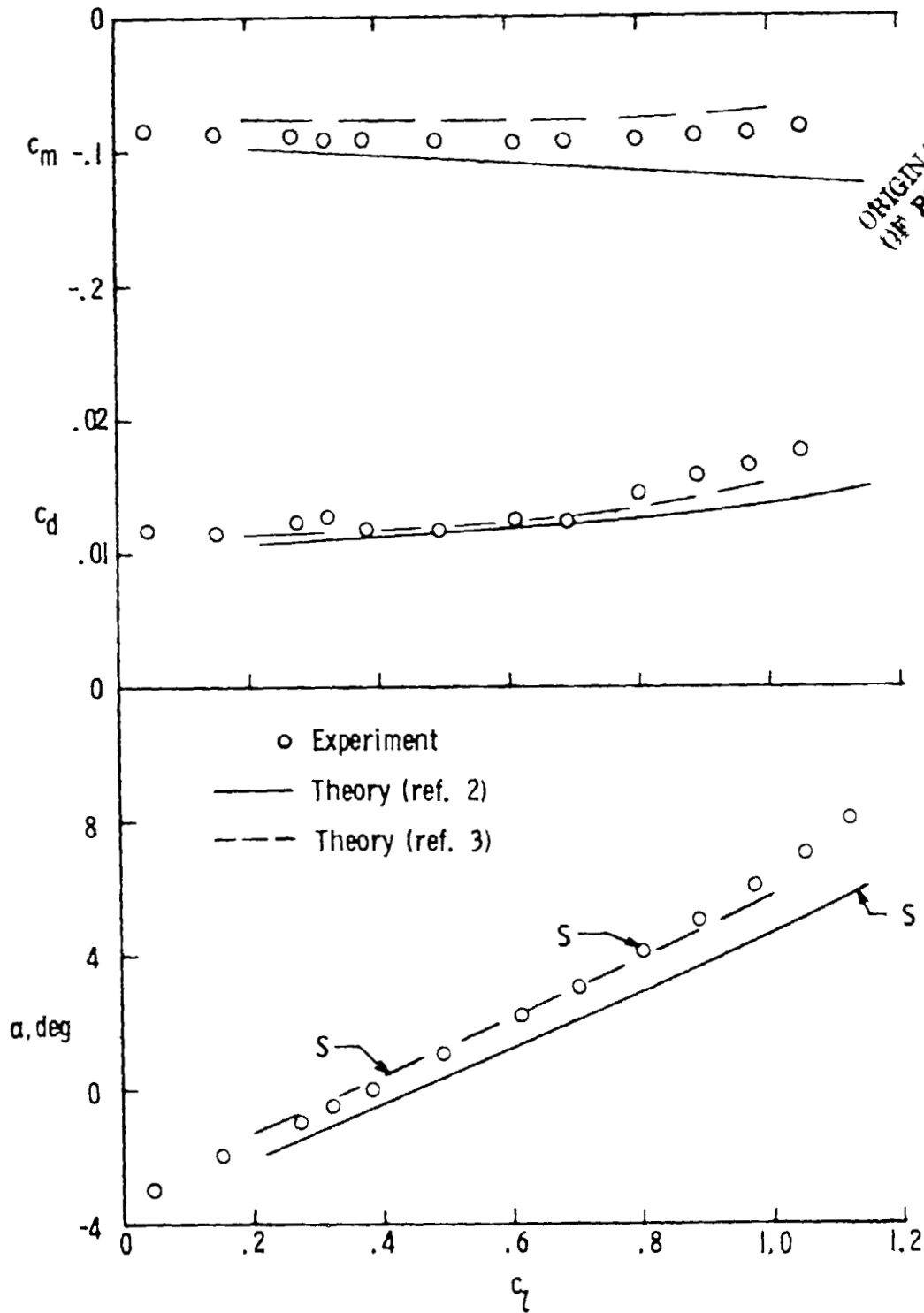
Figure 4.- Comparison of experimental and theoretical section data for
LS(1)-0421 airfoil. M = 0.15; R = 4.0 × 10^6; roughness on.

(a) $c_l = 0.40$.
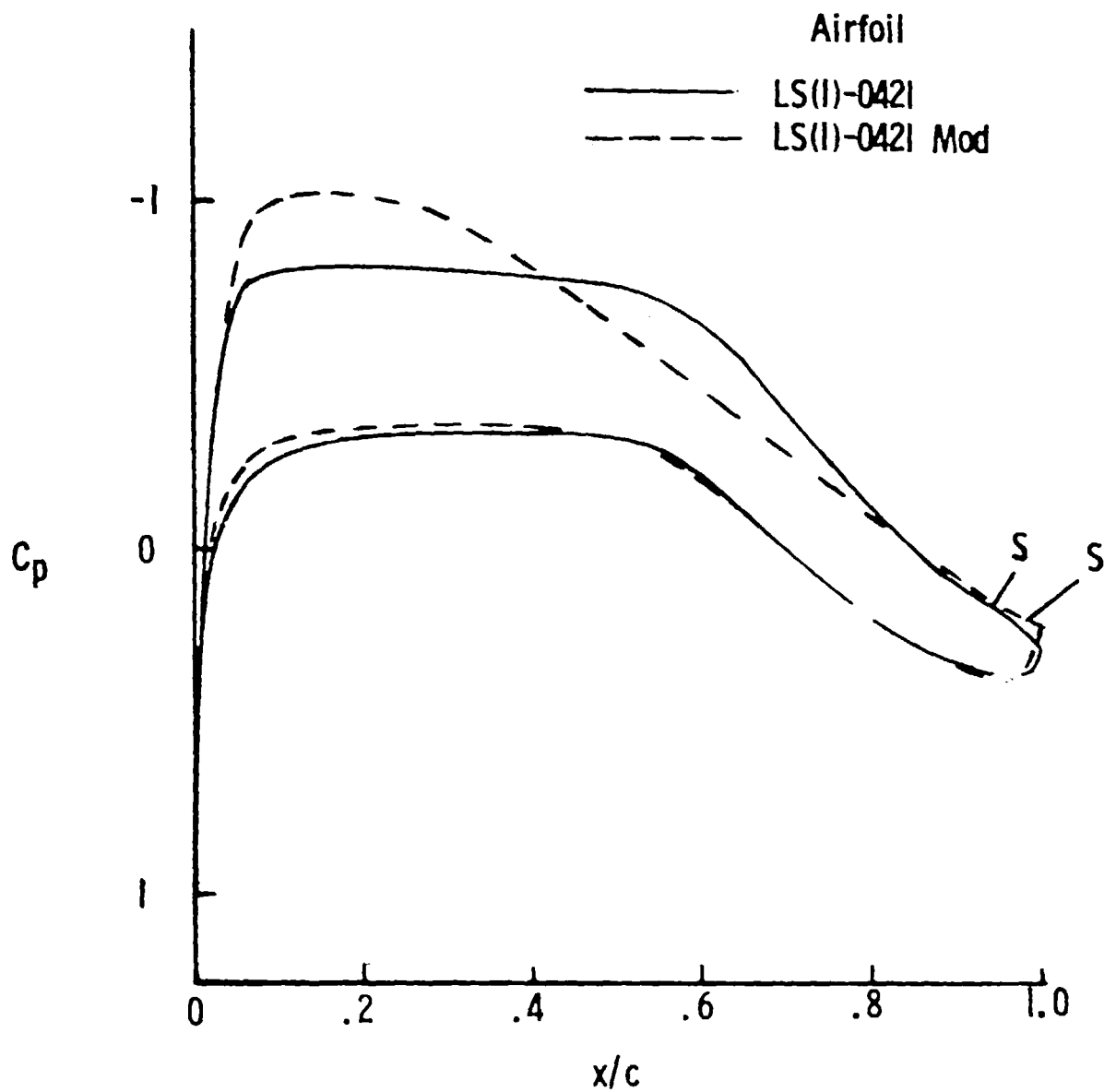
Figure 5.- Theoretical chordwise pressure distributions for LS(1)-0421 and LS(1)-0421 modified airfoils. $M = 0.15$; $R = 4.0 \times 10^6$.
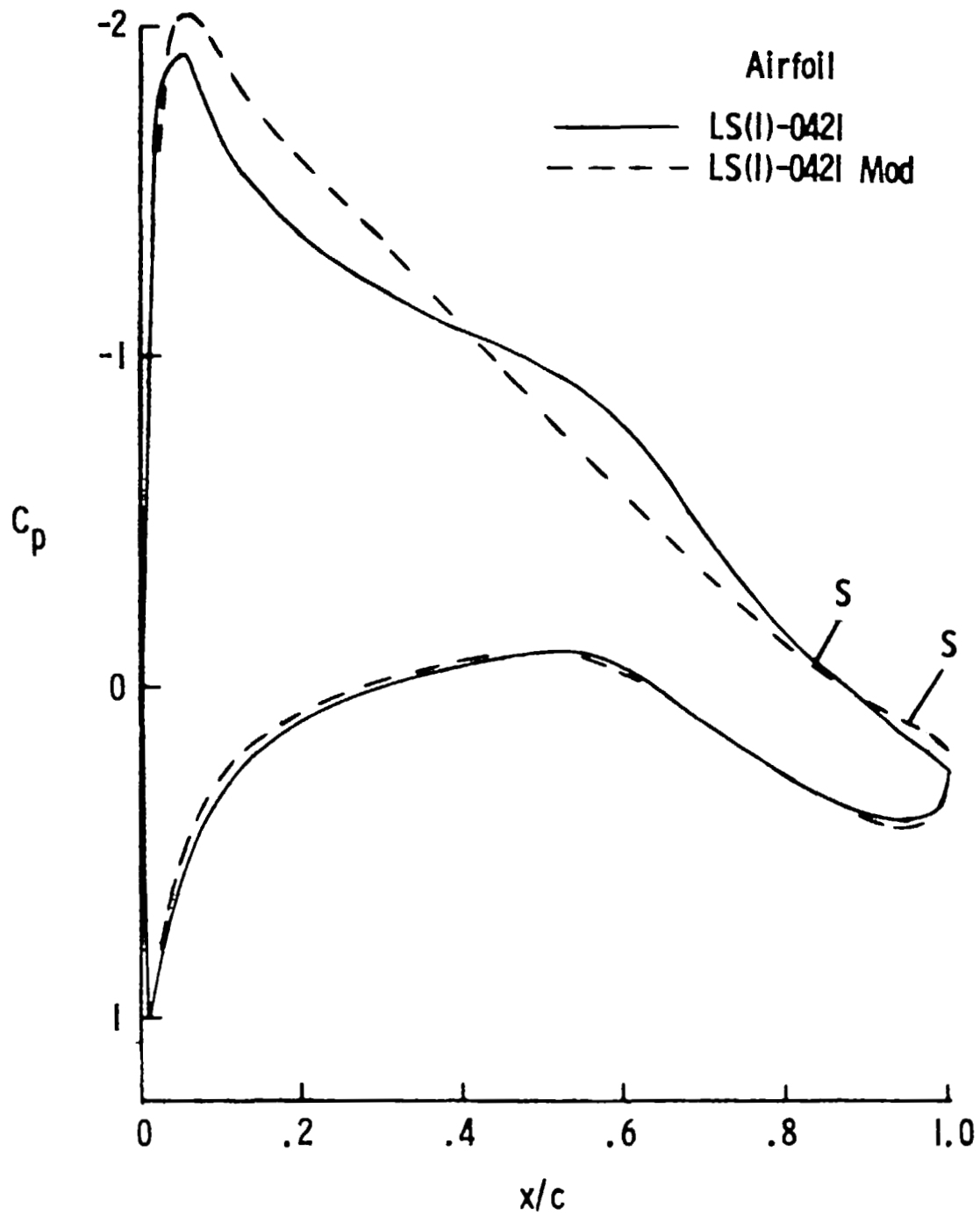
(b) $c_l = 1.0$.

Figure 5.- Concluded.
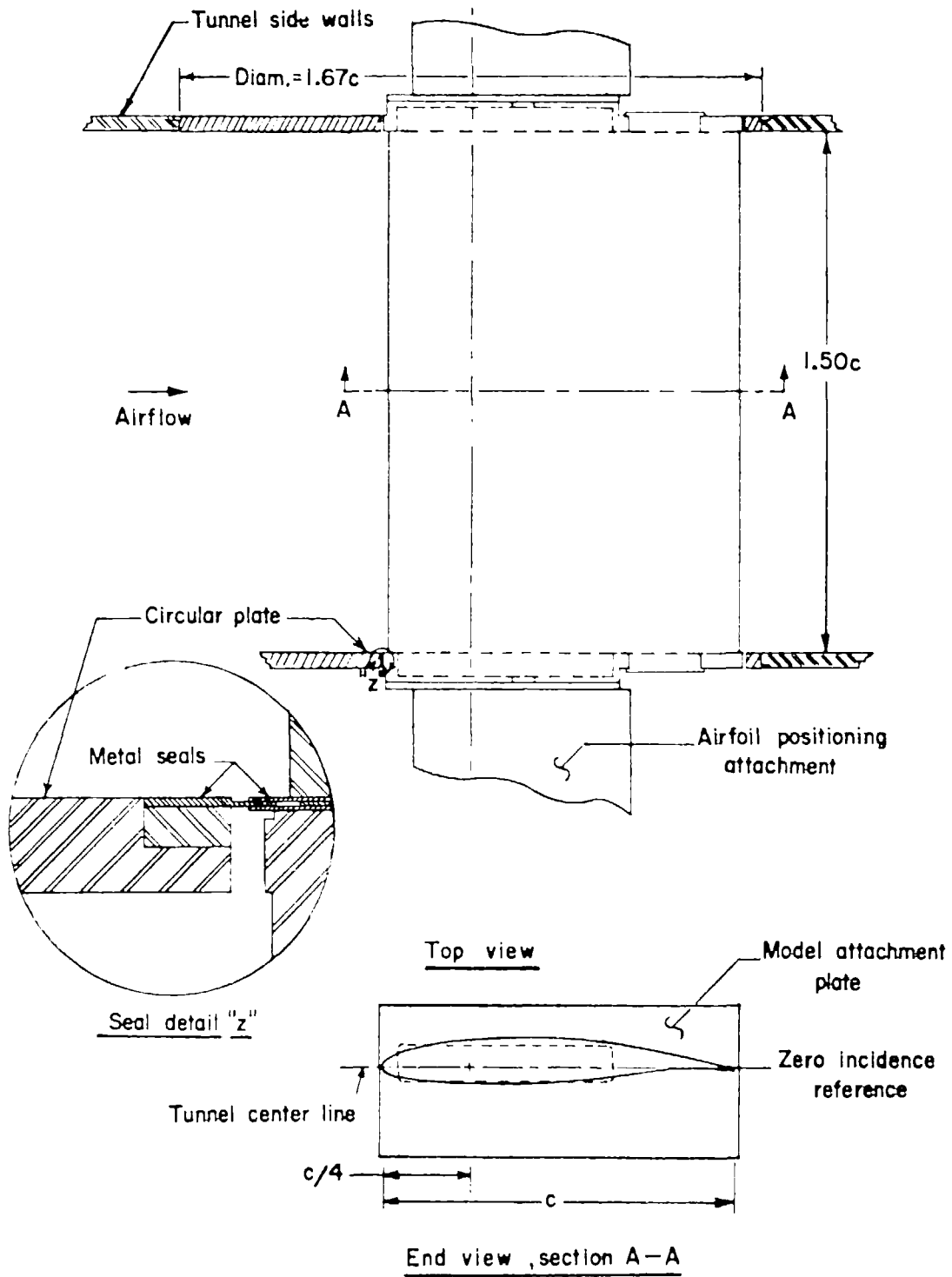
Figure 6.- Typical airfoil model mounted in wind tunnel. c = 61 cm (24 in.).
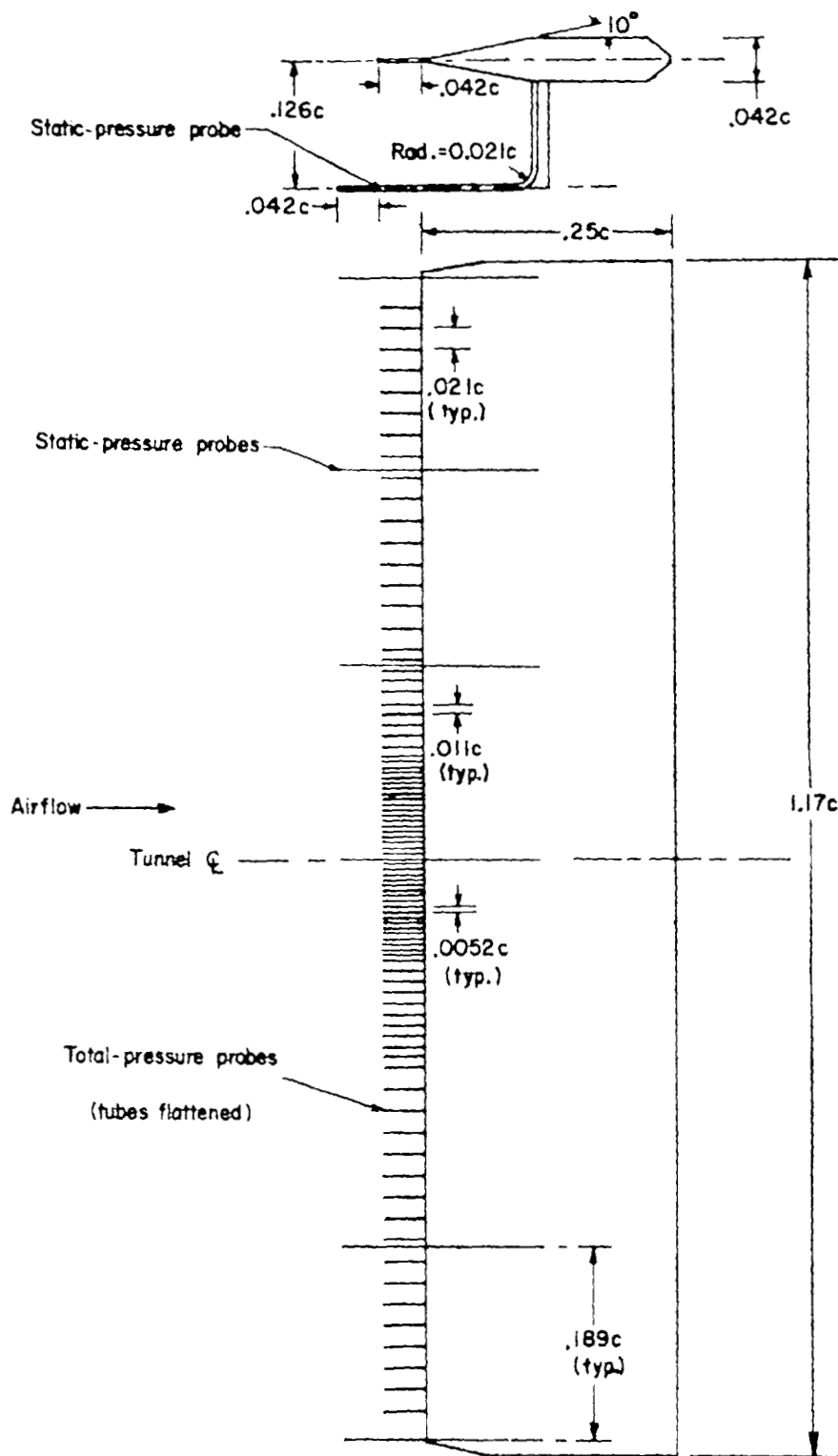
Figure 7.- Wake survey rake. c = 61 cm (24 in.).

18
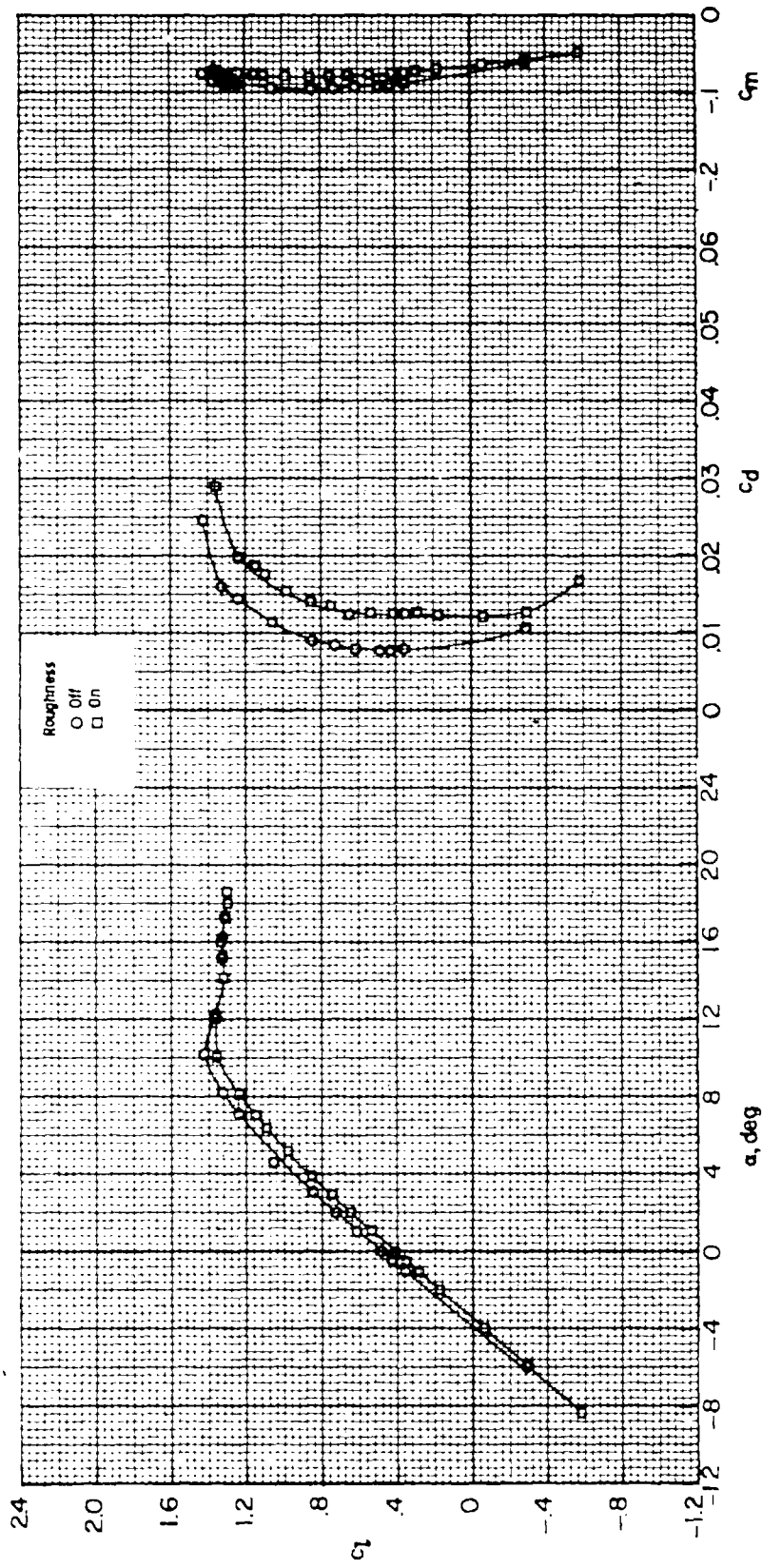
(a) $R = 2.0 \times 10^6$.

Figure 8.- Effect of Reynolds number on section characteristics for
LS(1)-0421 modified airfoil. $M = 0.15$.
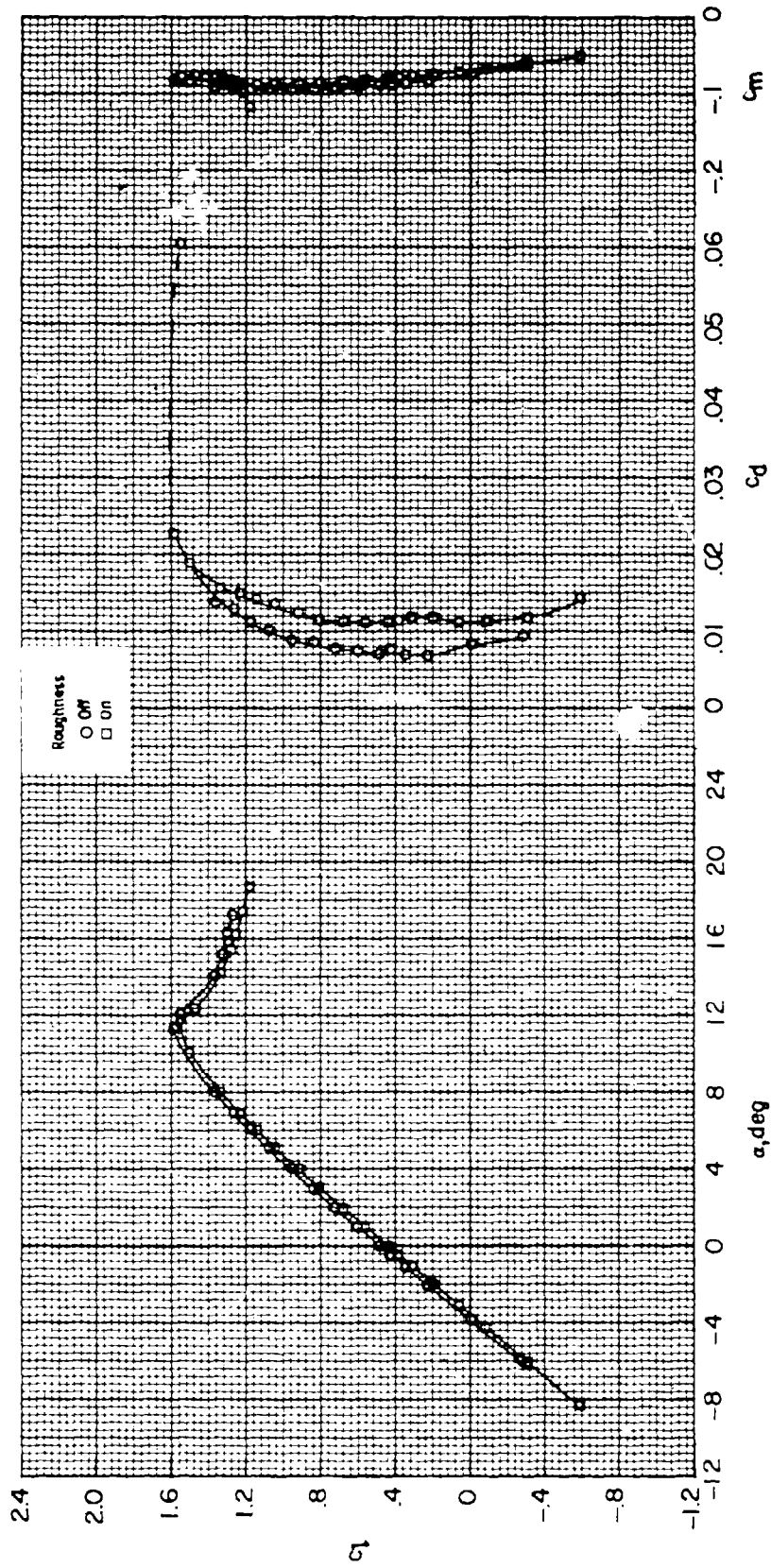
(b) R = 4.0 × 10⁶.

Figure 8.- Continued.
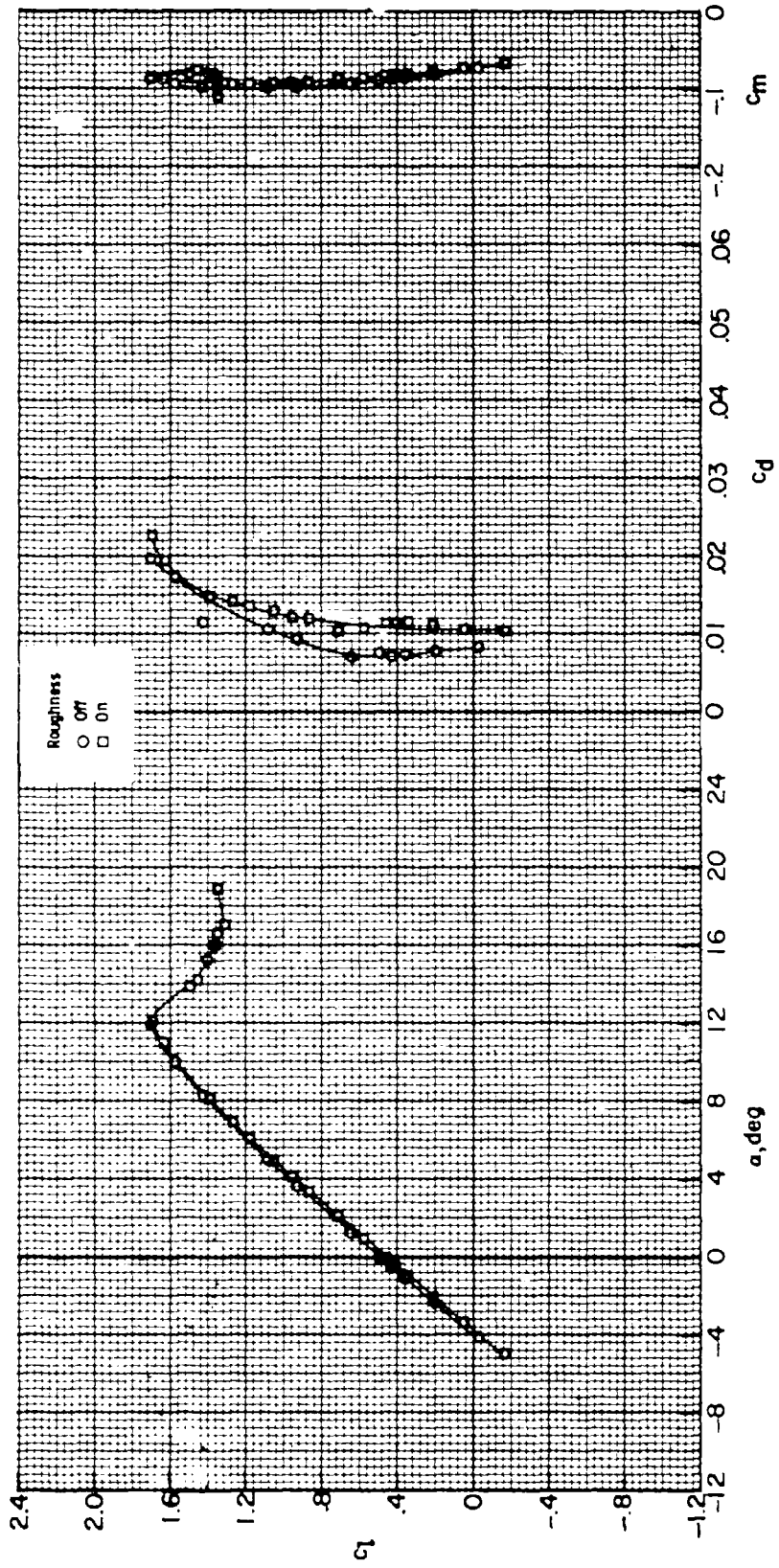
(a) R = 6.0 × 10⁶.

Figure 8.- Continued.
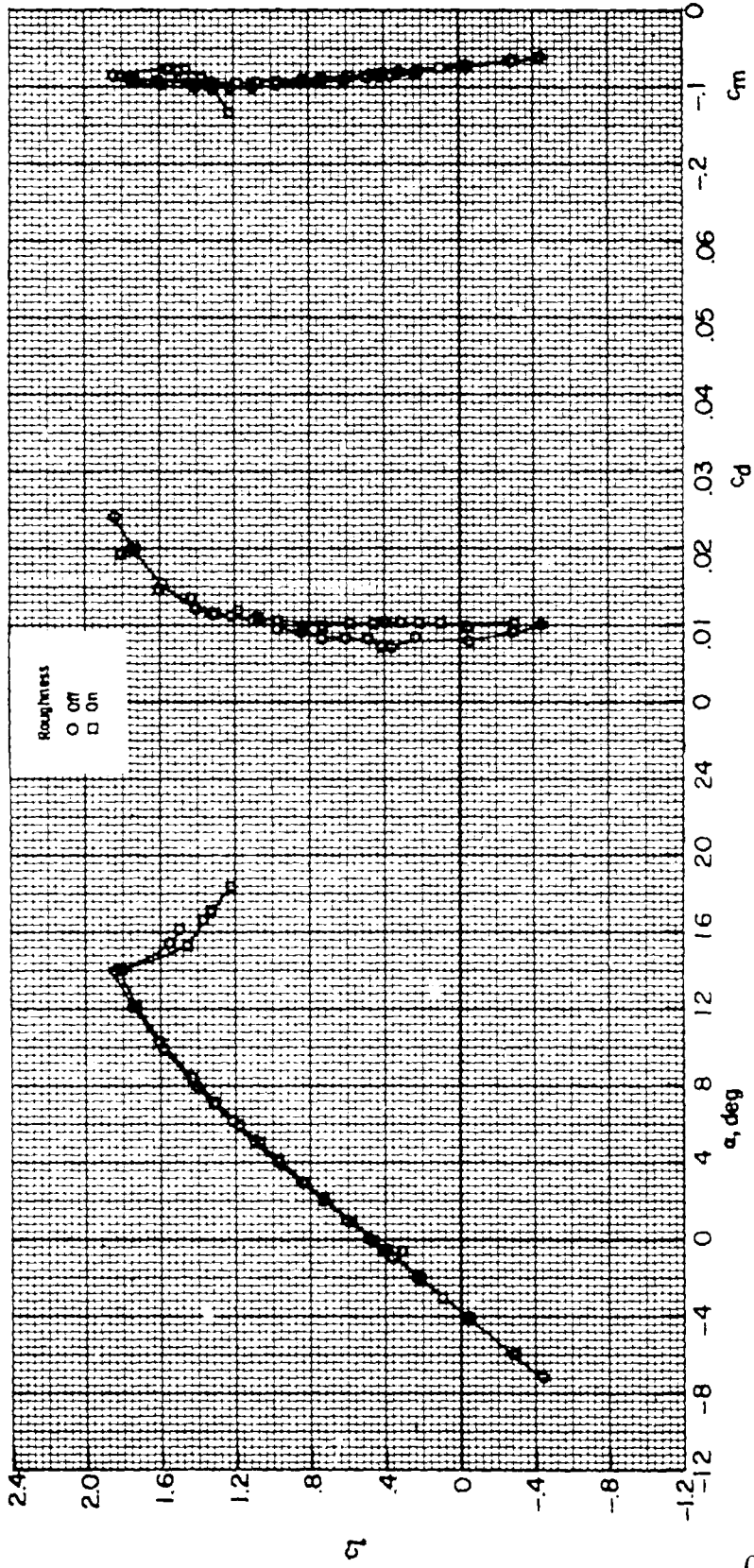
(d) $R = 9.0 \times 10^6$.

Figure 8.— Concluded.

22
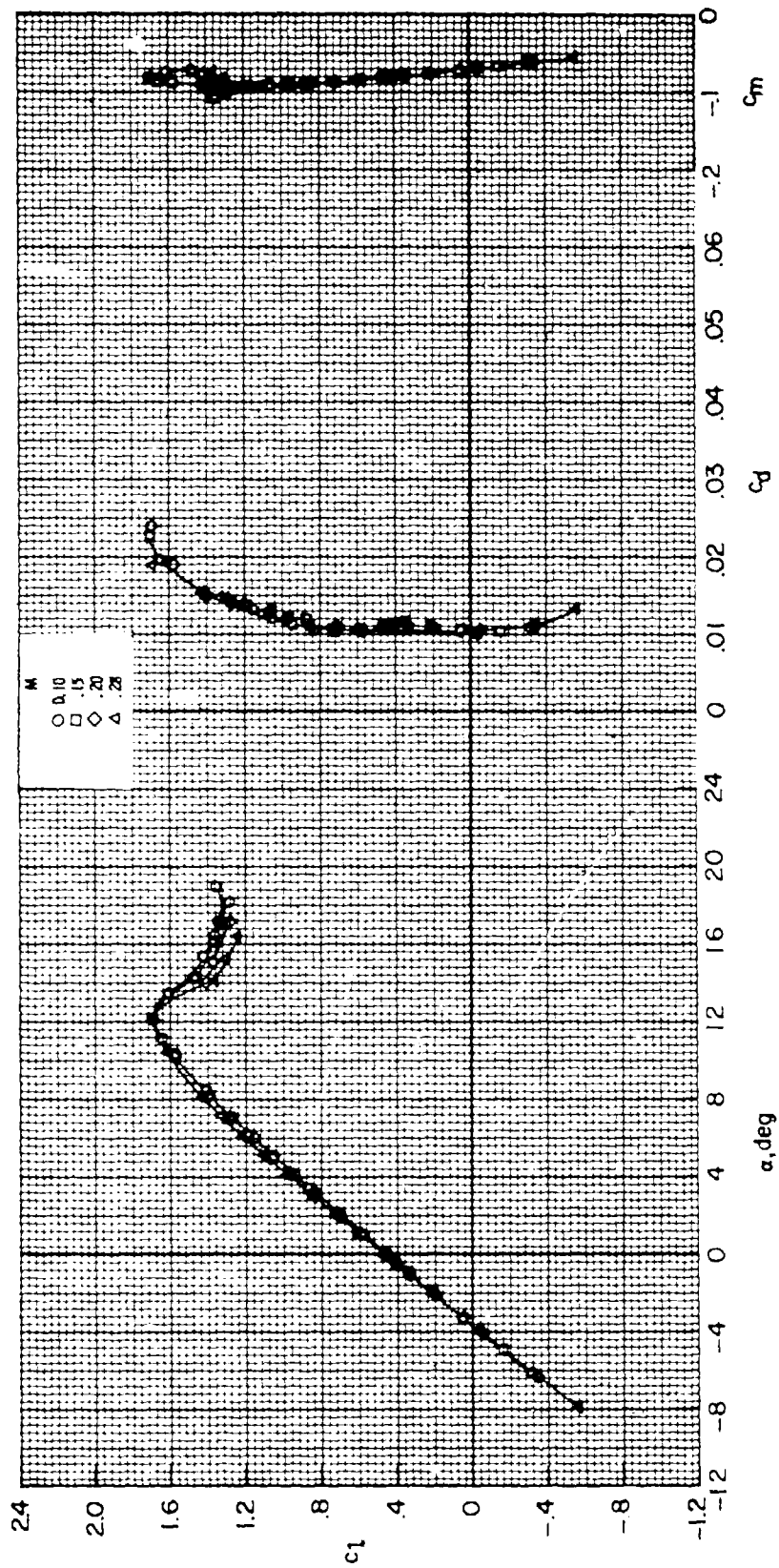
Figure 9.- Effect of free-stream Mach number on section characteristics for LS(1)-0421 modified airfoil. R = 6.0 × 10⁶; roughness on.
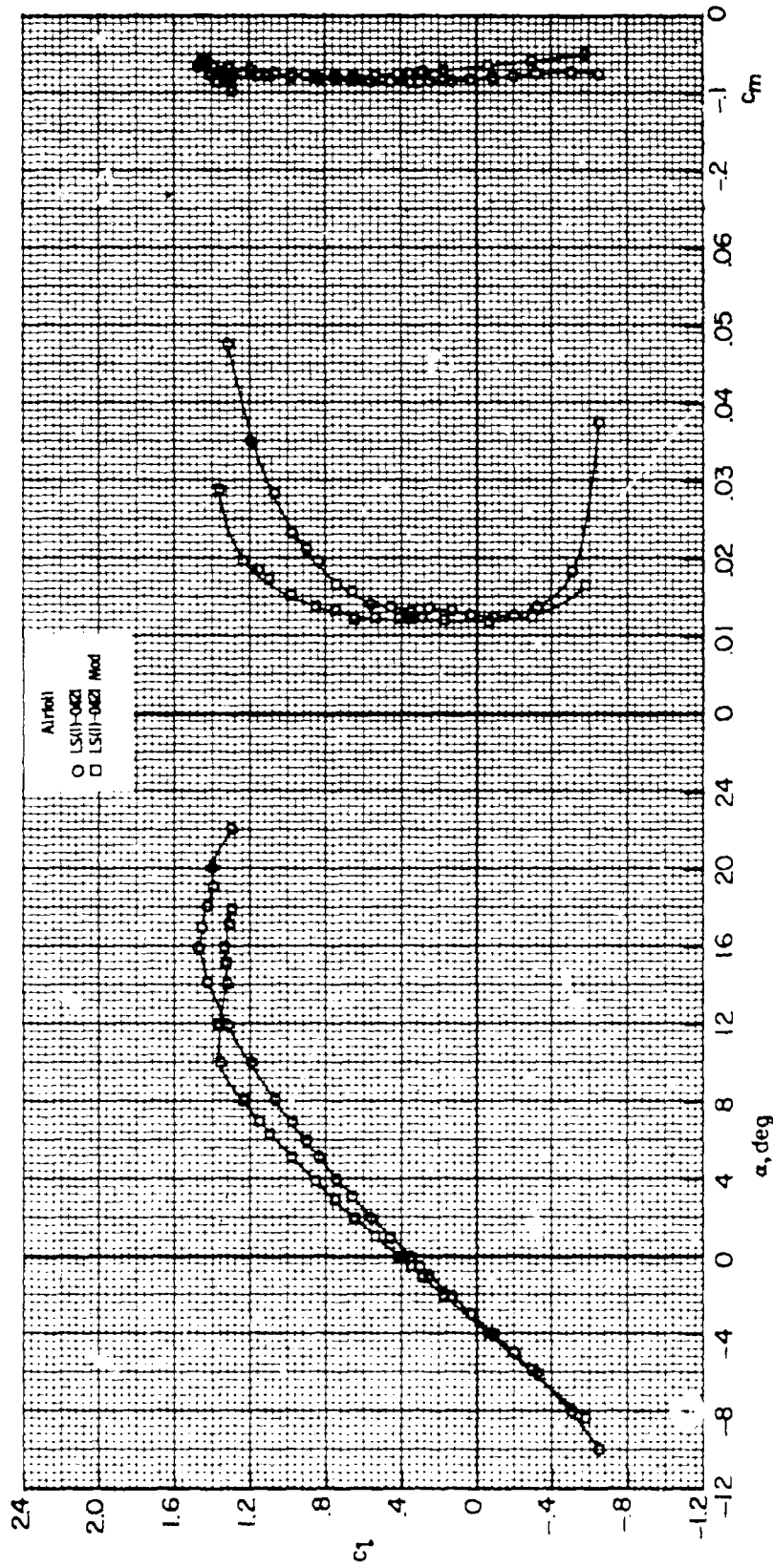
Figure 10.- Comparison of section characteristics for LS(1)-0421 and LS(1)-0421 modified airfoils. M = 0.15; roughness on.

(a) R = 2.0 × 10^6.

24
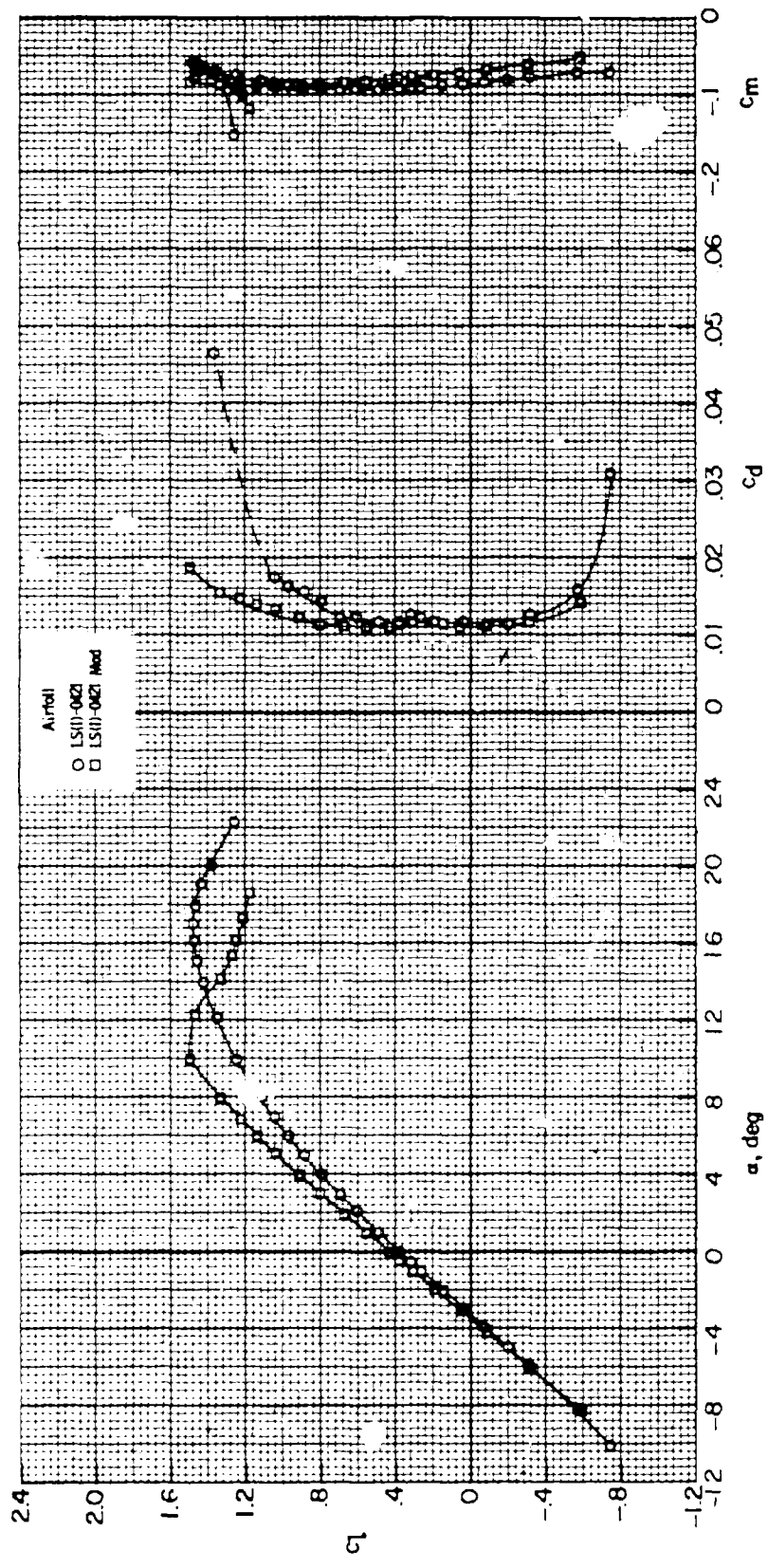
(b) $R = 4.0 \times 10^6$.

Figure 10.- Continued.
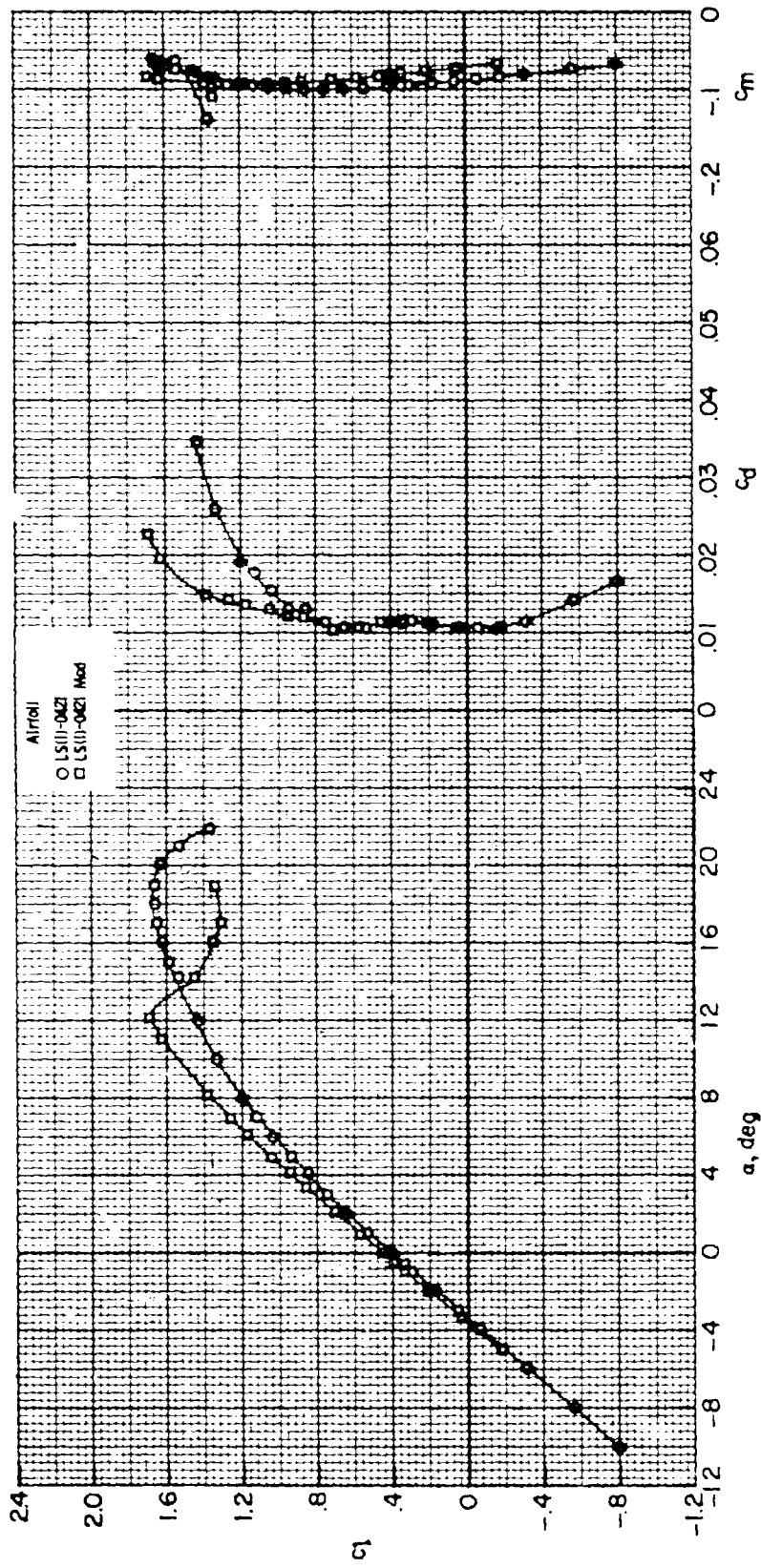
(a) $R = 6.0 \times 10^6$.

Figure 10.- Continued.
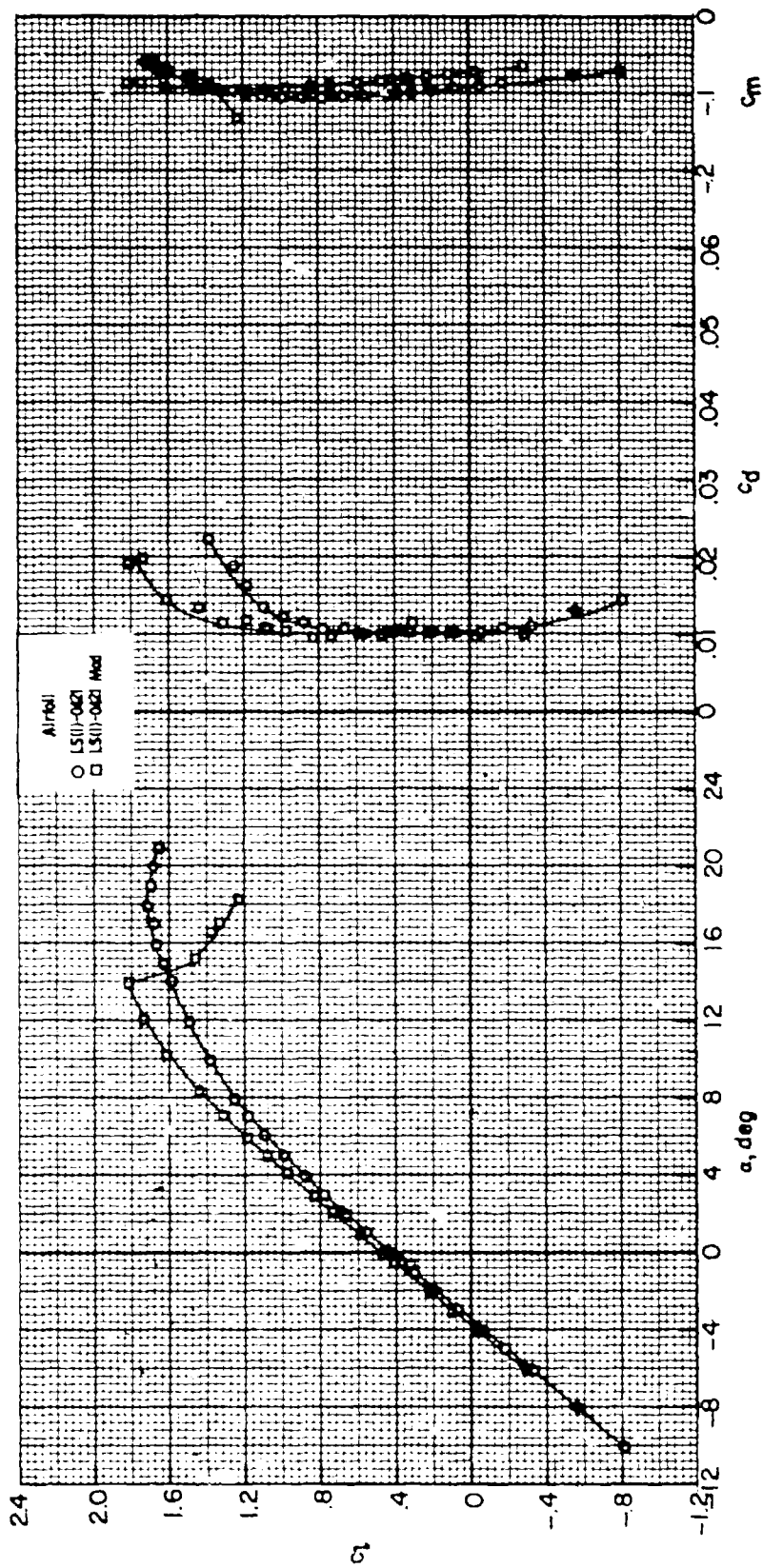
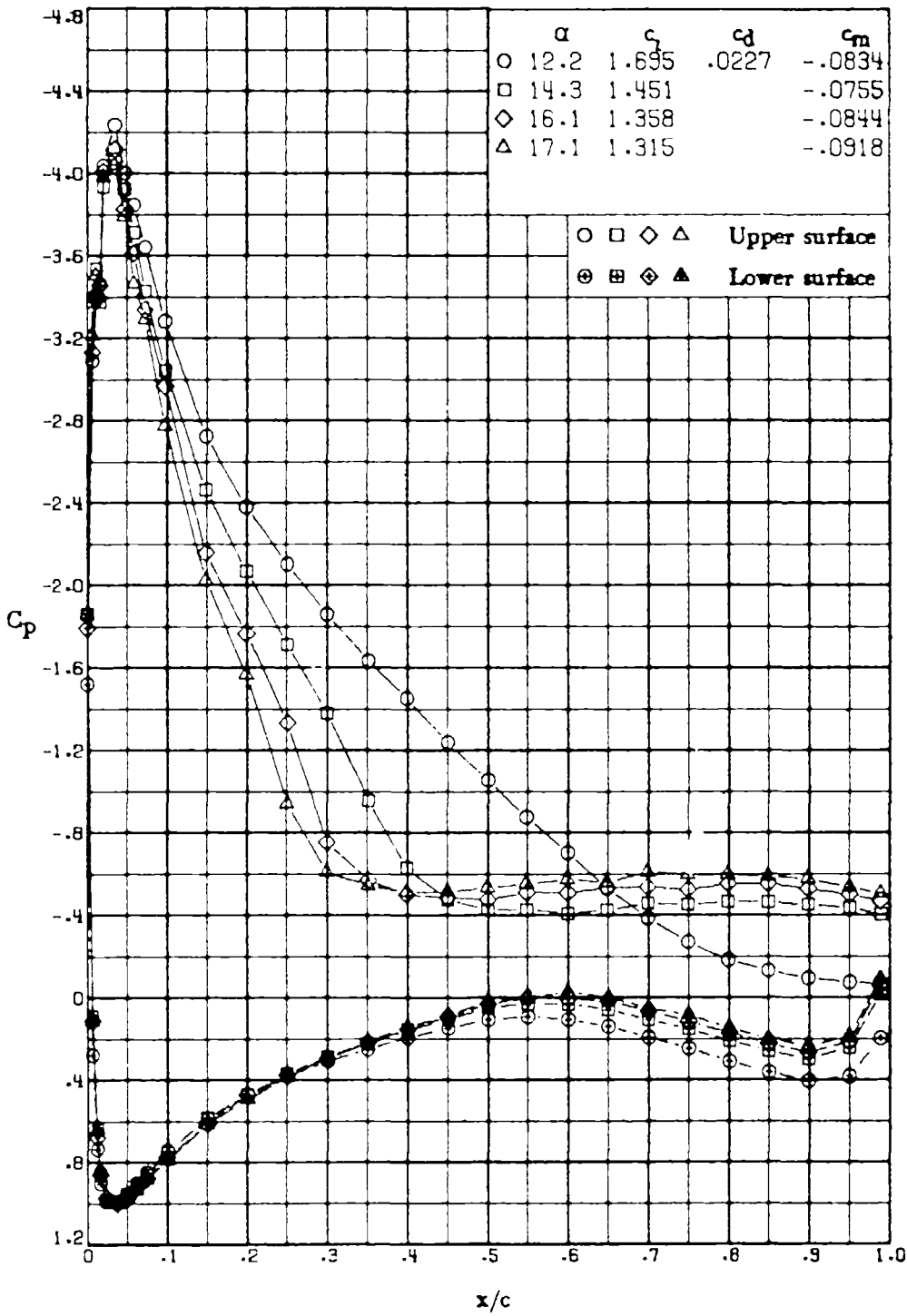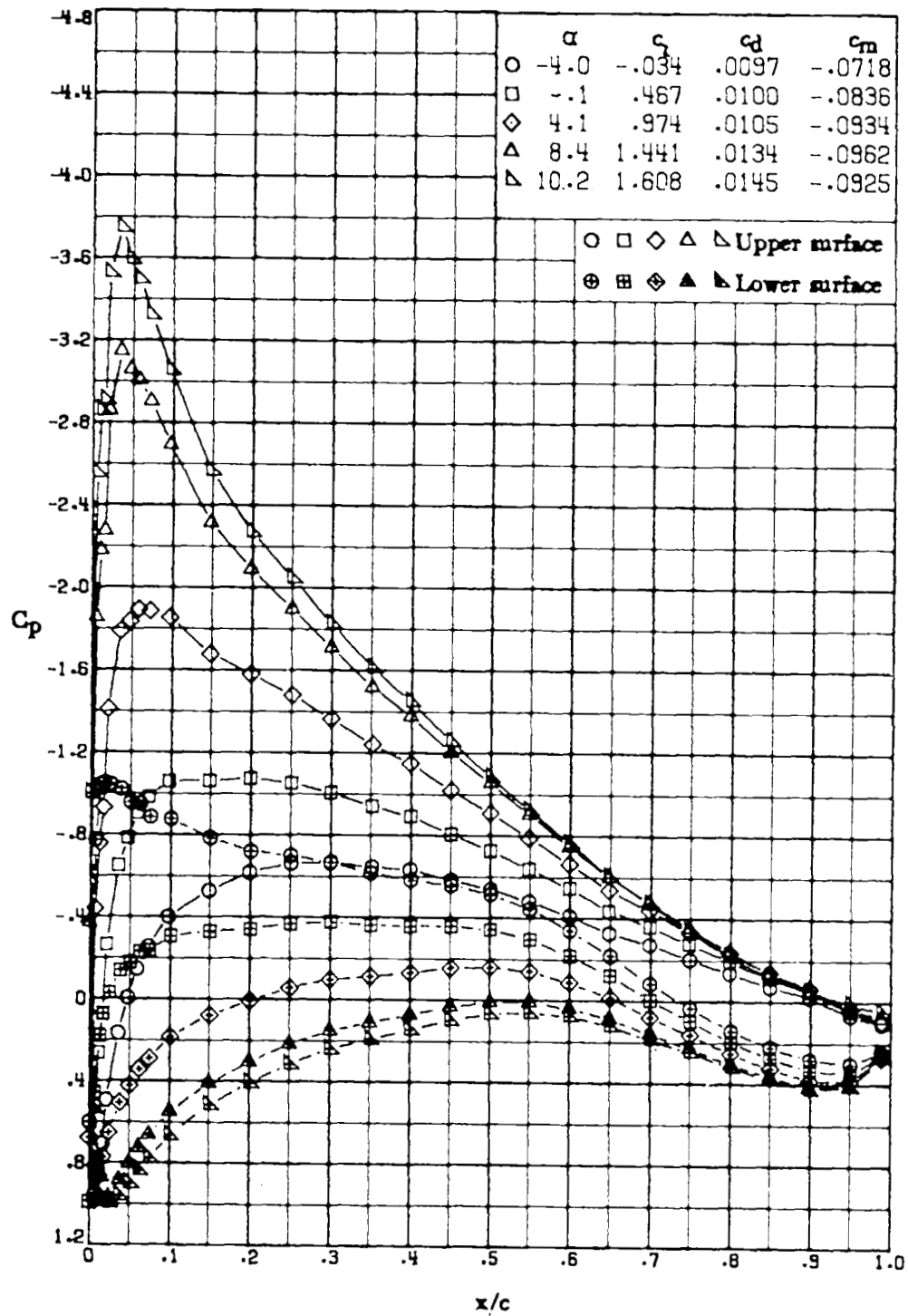(d) $R = 9.0 \times 10^6$.

Figure 10.- Concluded.
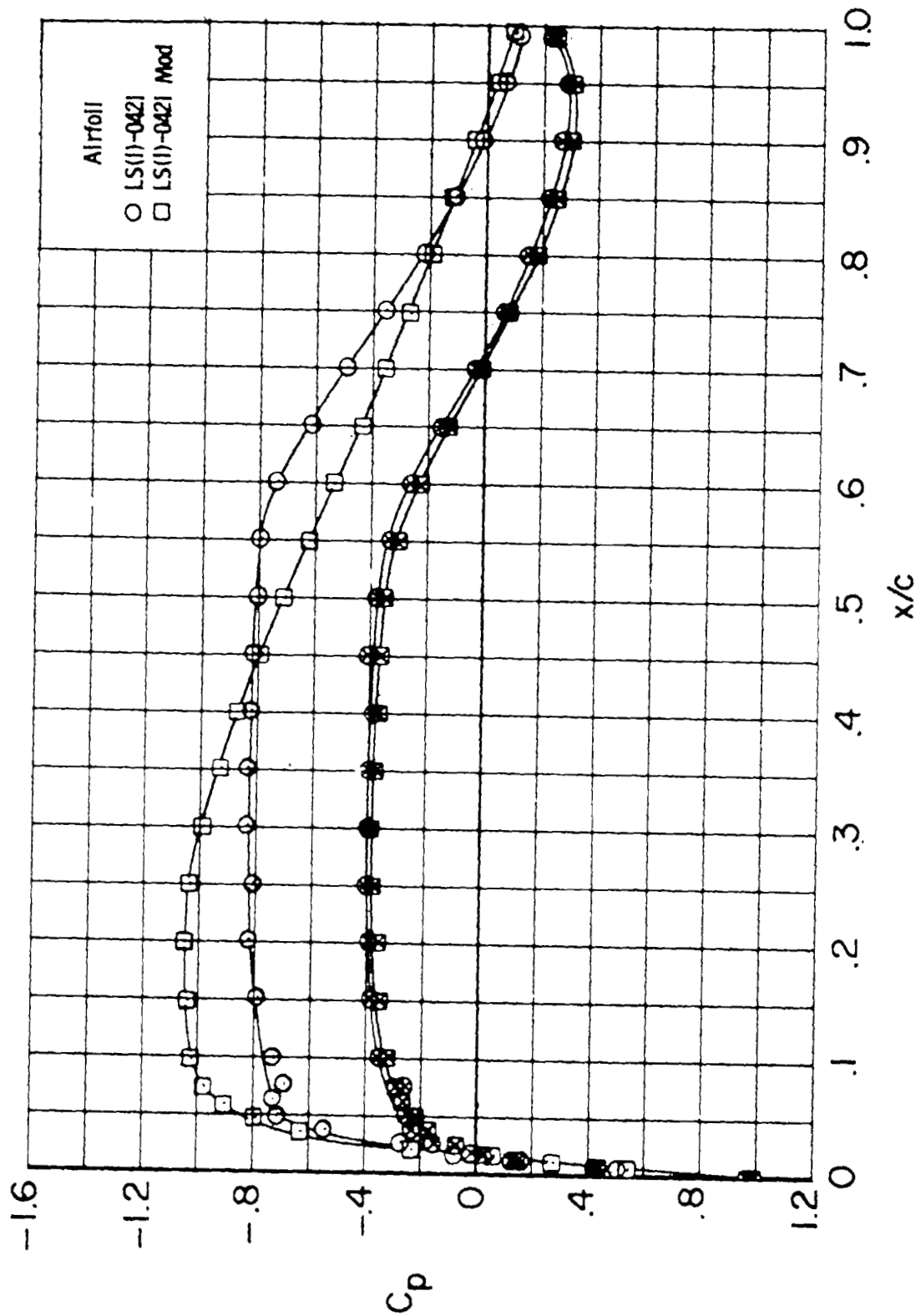
	α	c_l	c_d	c_m
○	-4.0	-.063	.0120	-.0641
□	0.0	.416	.0124	-.0751
◇	3.9	.855	.0140	-.0736
△	8.1	1.239	.0198	-.0743
◮	10.1	1.361	.0290	-.0749

○ □ ◇ △ ◮ Upper surface

⊕ ⊞ ◈ ▲ ◣ Lower surface
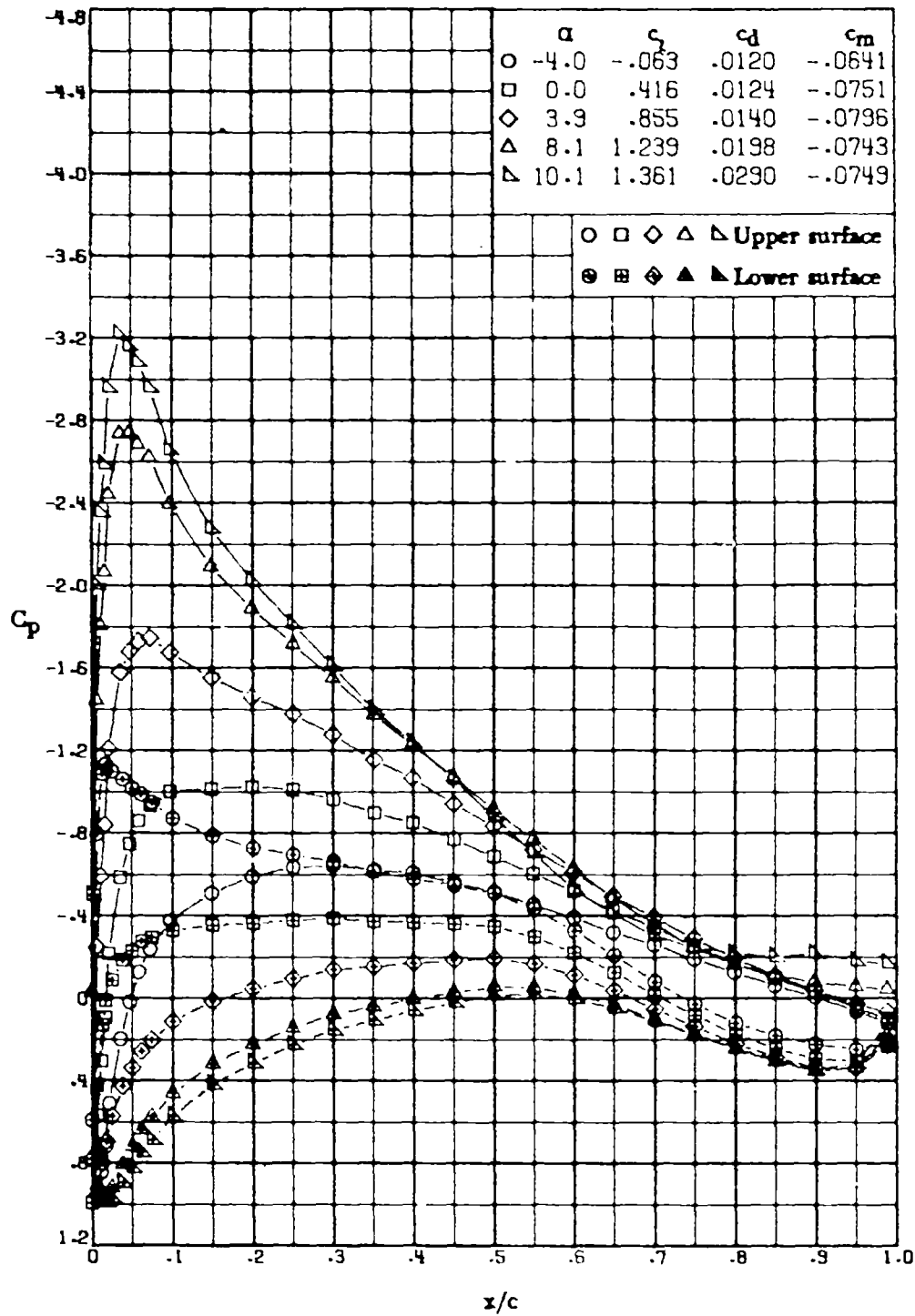
(a) $R = 2.0 \times 10^6$.

Figure 11.- Effect of Reynolds number on chordwise pressure distributions for LS(')-0421 modified airfoil. M = 0.15; roughness on.

	α	c_l	c_d	c_m
○	12.1	1.367		-.0851
□	14.2	1.319		-.0756
◇	15.3	1.325		-.0758
△	18.0	1.295		-.0871

| ○ □ ◇ △ | Upper surface |
| ⬤ ▣ ◆ ▲ | Lower surface |

(a) $R \approx 2.0 \times 10^6$. Concluded.

Figure 11.- Continued.

	α	c_l	c_d	c_m
O	-3.1	.063	.0111	-.0706
□	0.0	.440	.0111	-.0730
◇	4.0	.919	.0124	-.0868
△	8.0	1.336	.0156	-.0864
◺	10.1	1.497	.0189	-.0824

O □ ◇ △ ◺ Upper surface
⊕ ⊞ ◈ ▲ ◣ Lower surface
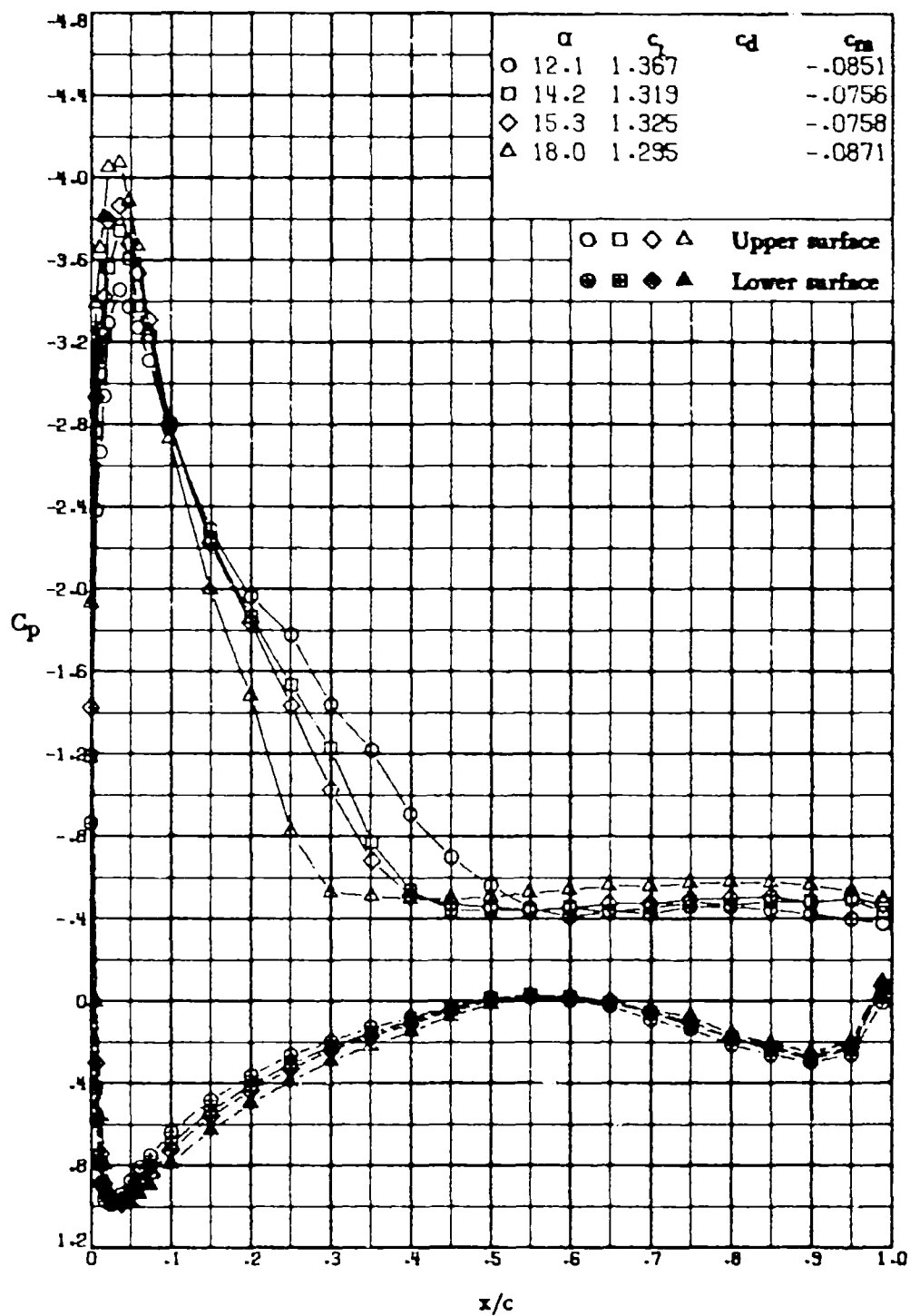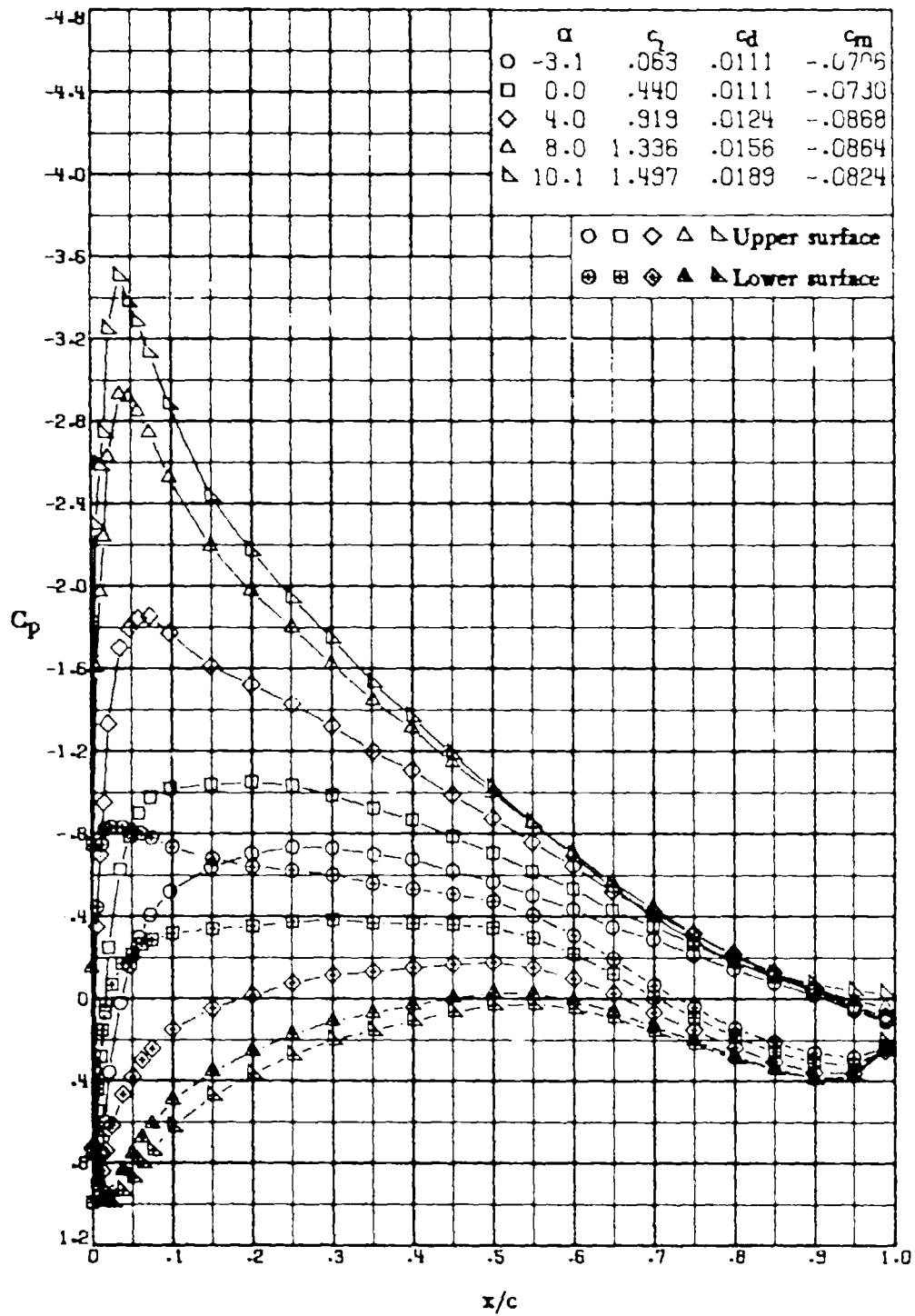
(b) $R = 4.0 \times 10^6$.

Figure 11.- Continued.

(b) R = 4.0 × 10⁶. Concluded.
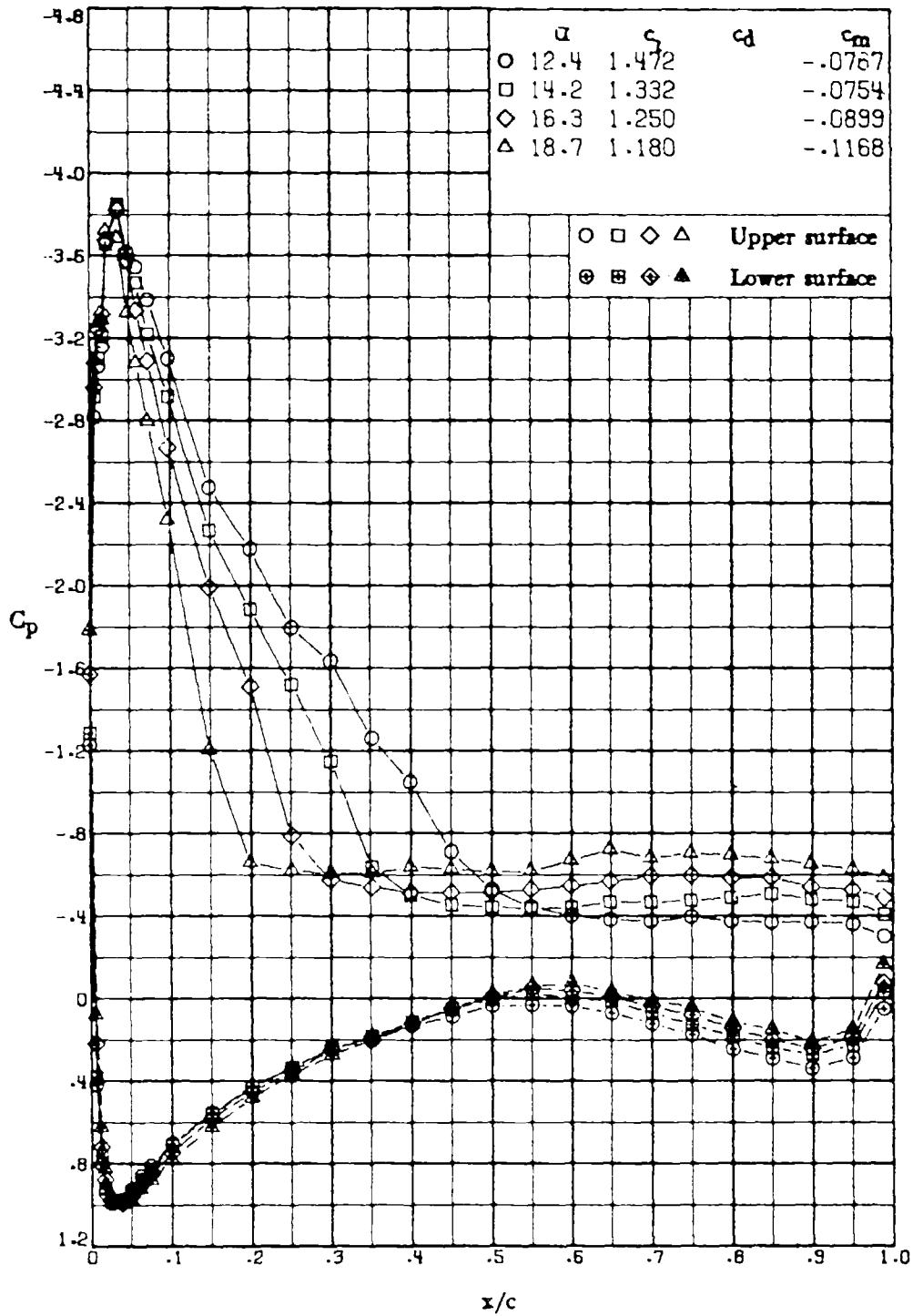
Figure 11.- Continued.
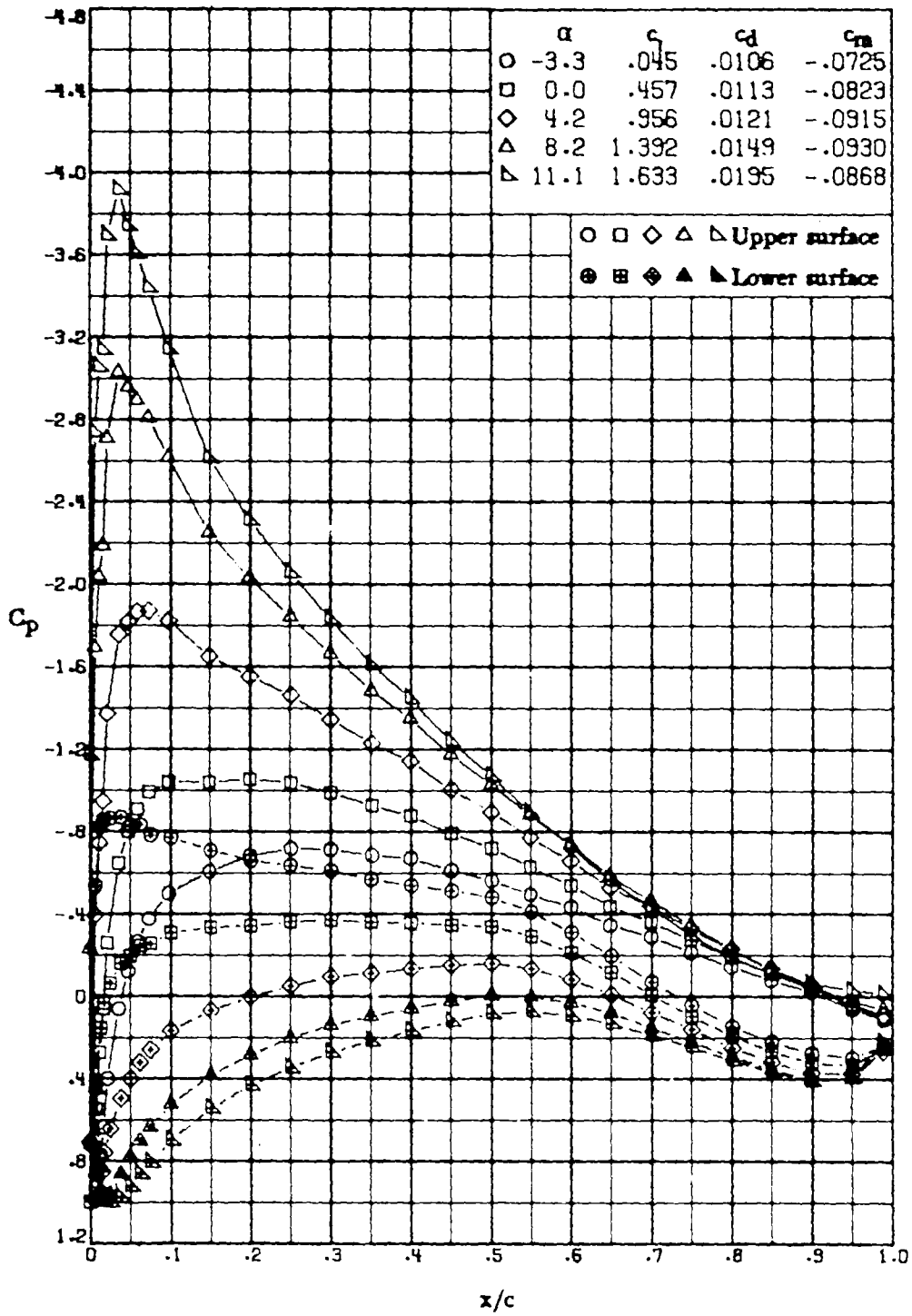
(c) R = 6.0 × 10⁶.

Figure 11.- Continued.

(c) R = 6.0 × 10^6. Concluded.

Figure 11.- Continued.

	α	c_l	c_d	c_m
O	-4.0	-.034	.0097	-.0718
□	-.1	.467	.0100	-.0836
◇	4.1	.974	.0105	-.0934
△	8.4	1.441	.0134	-.0962
◁	10..2	1.608	.0145	-.0925

O □ ◇ △ ◁ Upper surface

⊕ ⊞ ◈ ▲ ◣ Lower surface

(d) $R = 9.0 \times 10^6$.

Figure 11.- Continued.

34
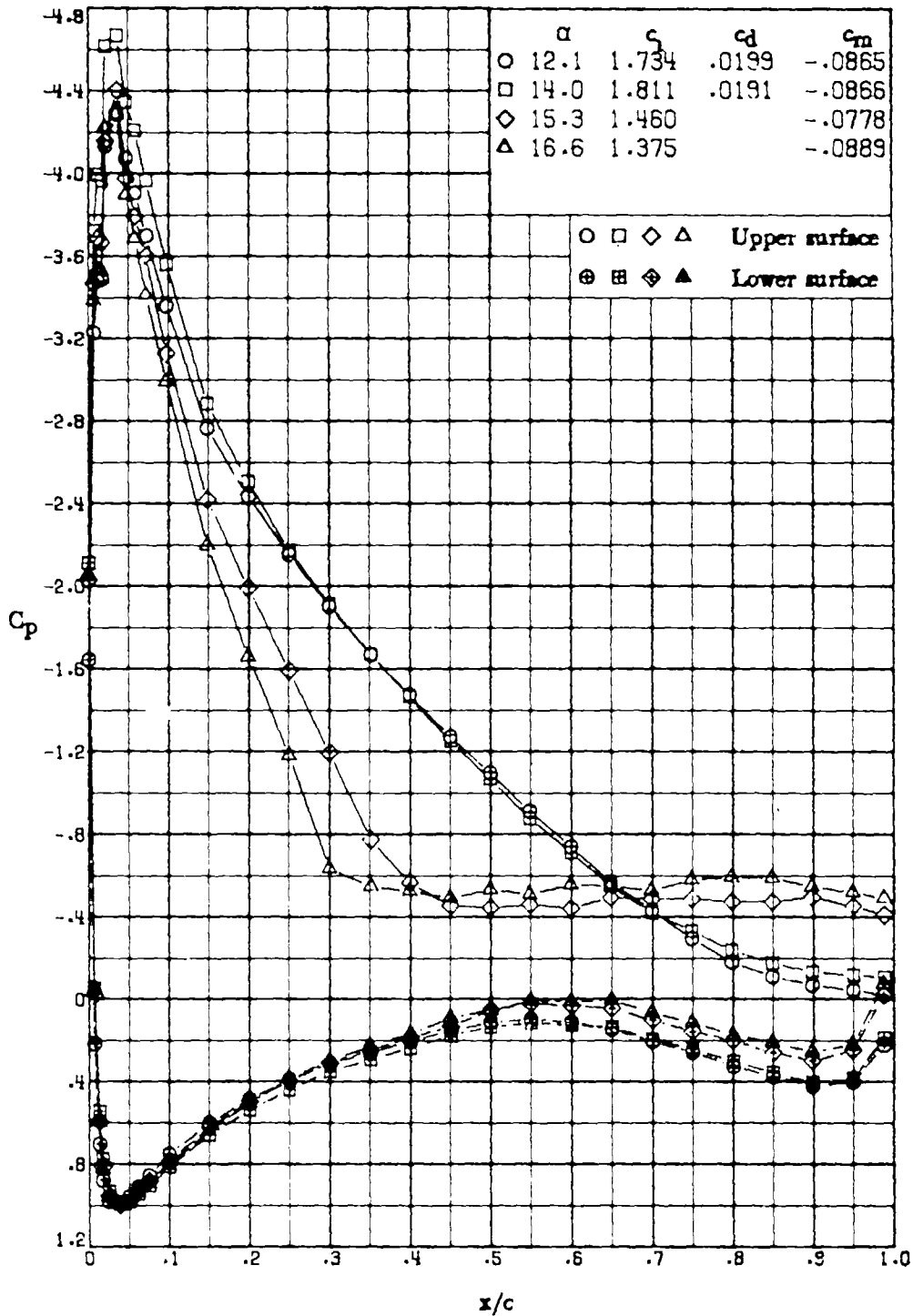
(d) R = 9.0 × 10⁶. Concluded.

Figure 11.- Concluded.

Figure 12.- Comparison of chordwise pressure distributions for LS(1)-0421 and LS(1)-042' modi-
fied airfoils. M = 0.15; roughness on. (Center-crossed symbols designate lower surface.)
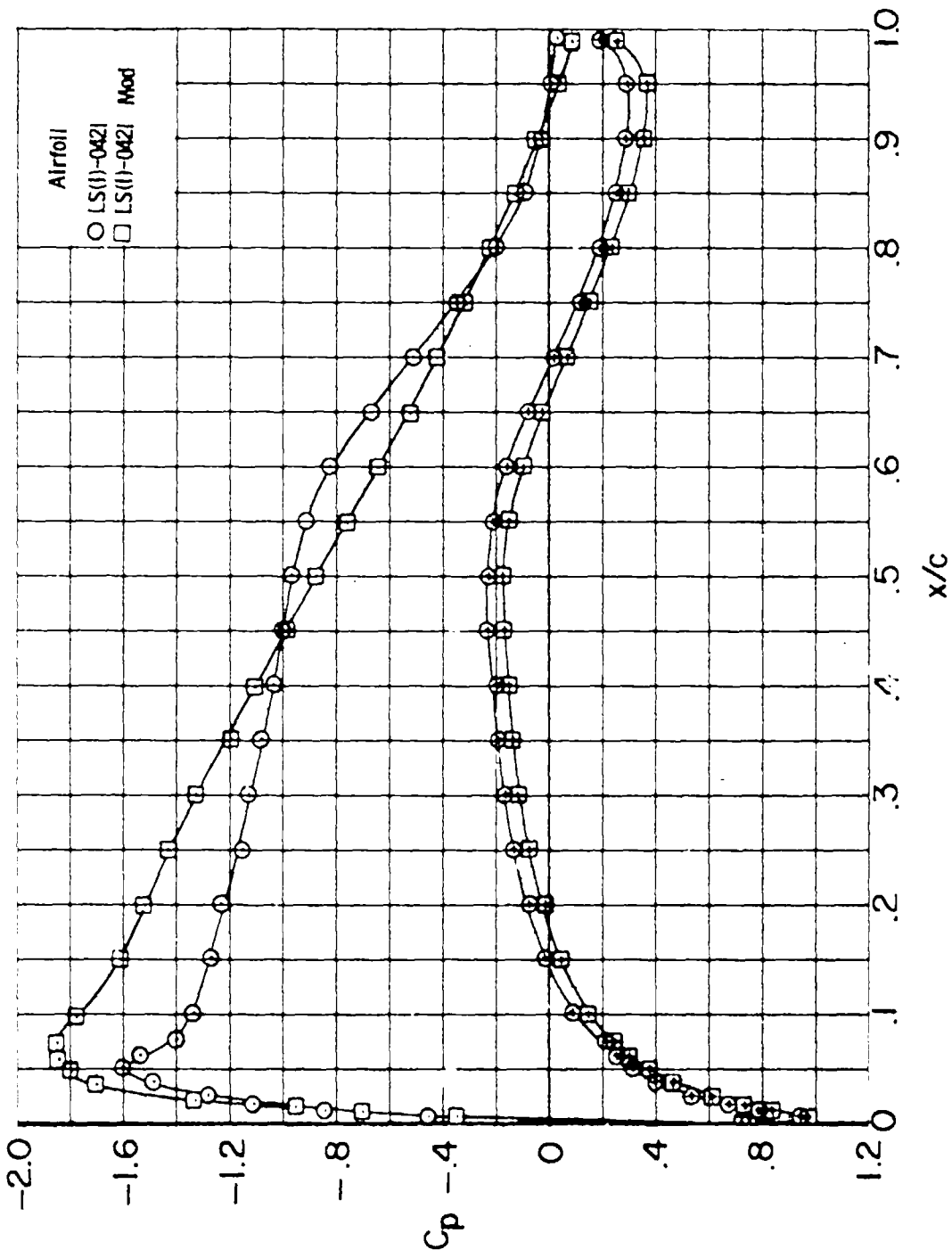
(a) $\alpha \approx 0°$; R = 4.0 × 10^{6}.

(b) $\alpha \approx 4^\circ$; $R = 4.0 \times 10^6$.

Figure 12.- Continued.
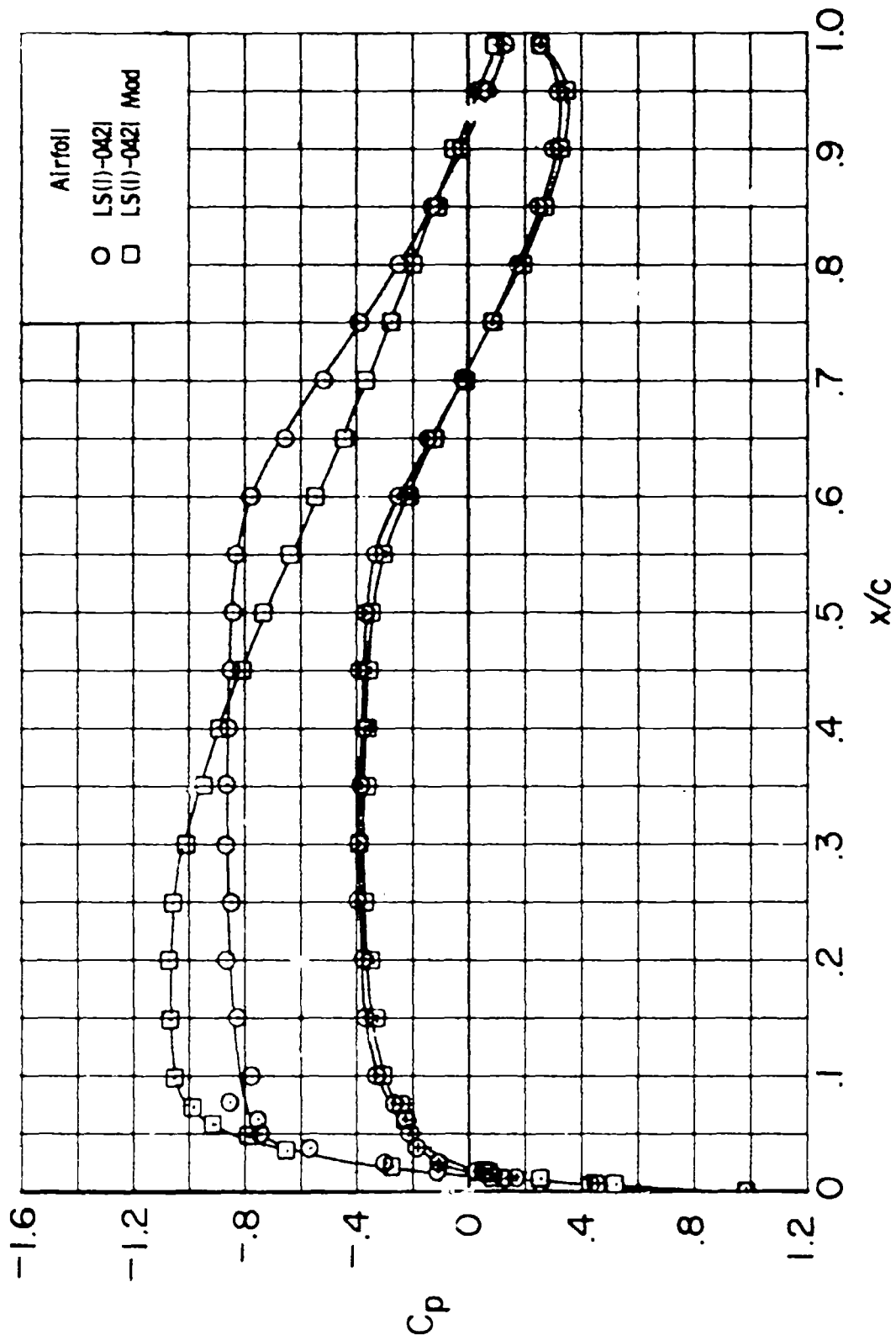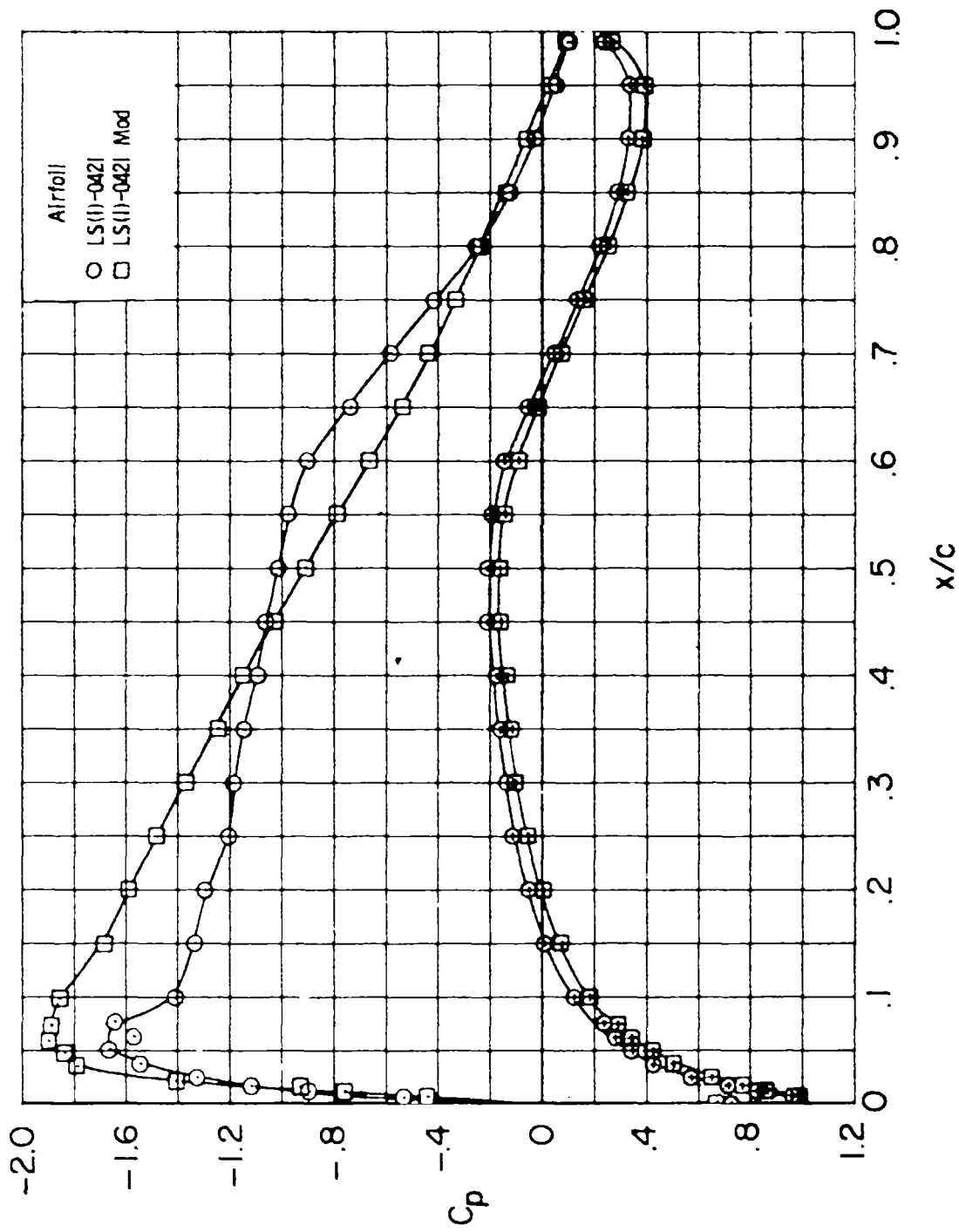
37
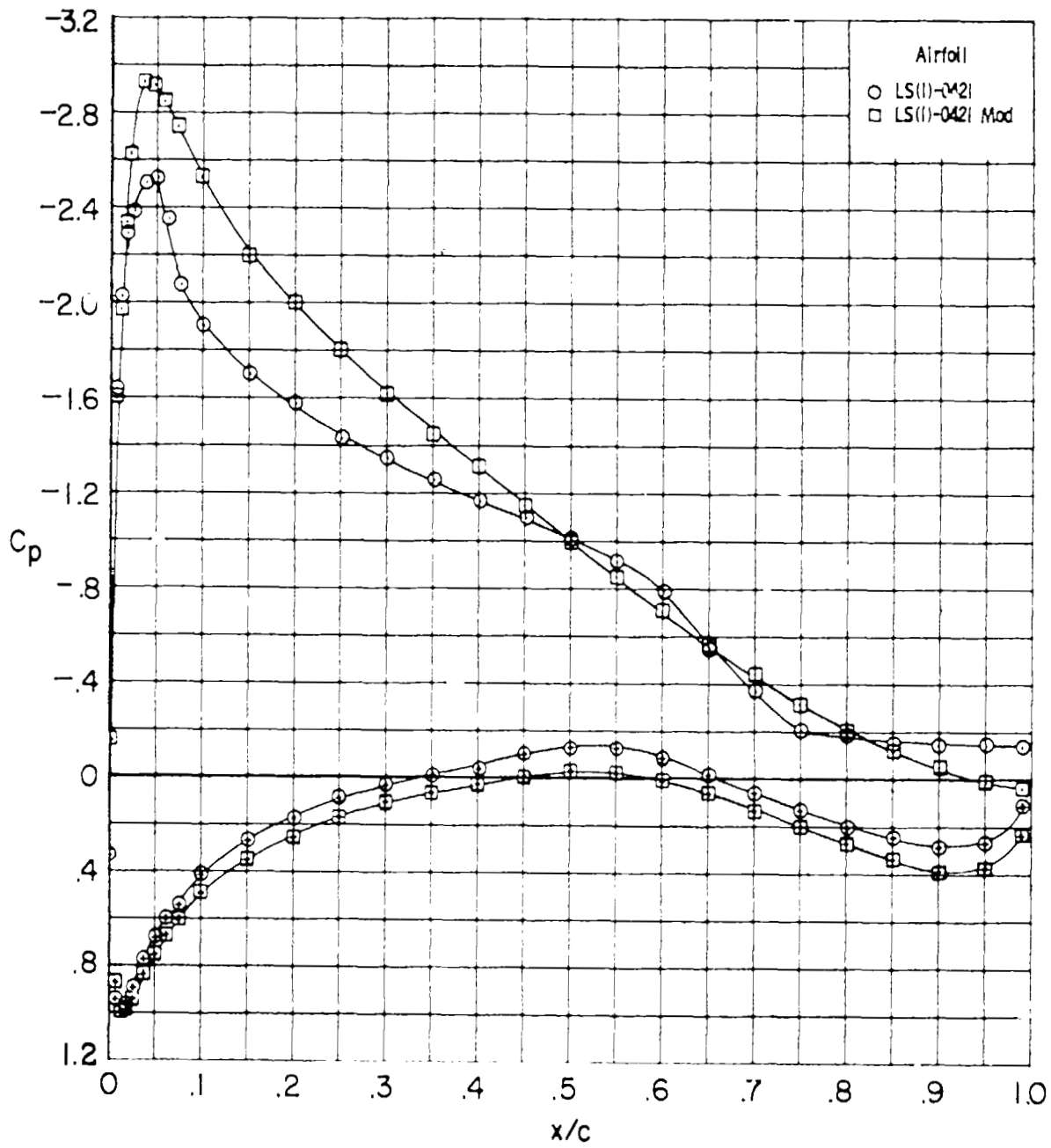
(c) $\alpha \approx 8°$; $R = 4.0 \times 10^6$.

Figure 12.- Continued.
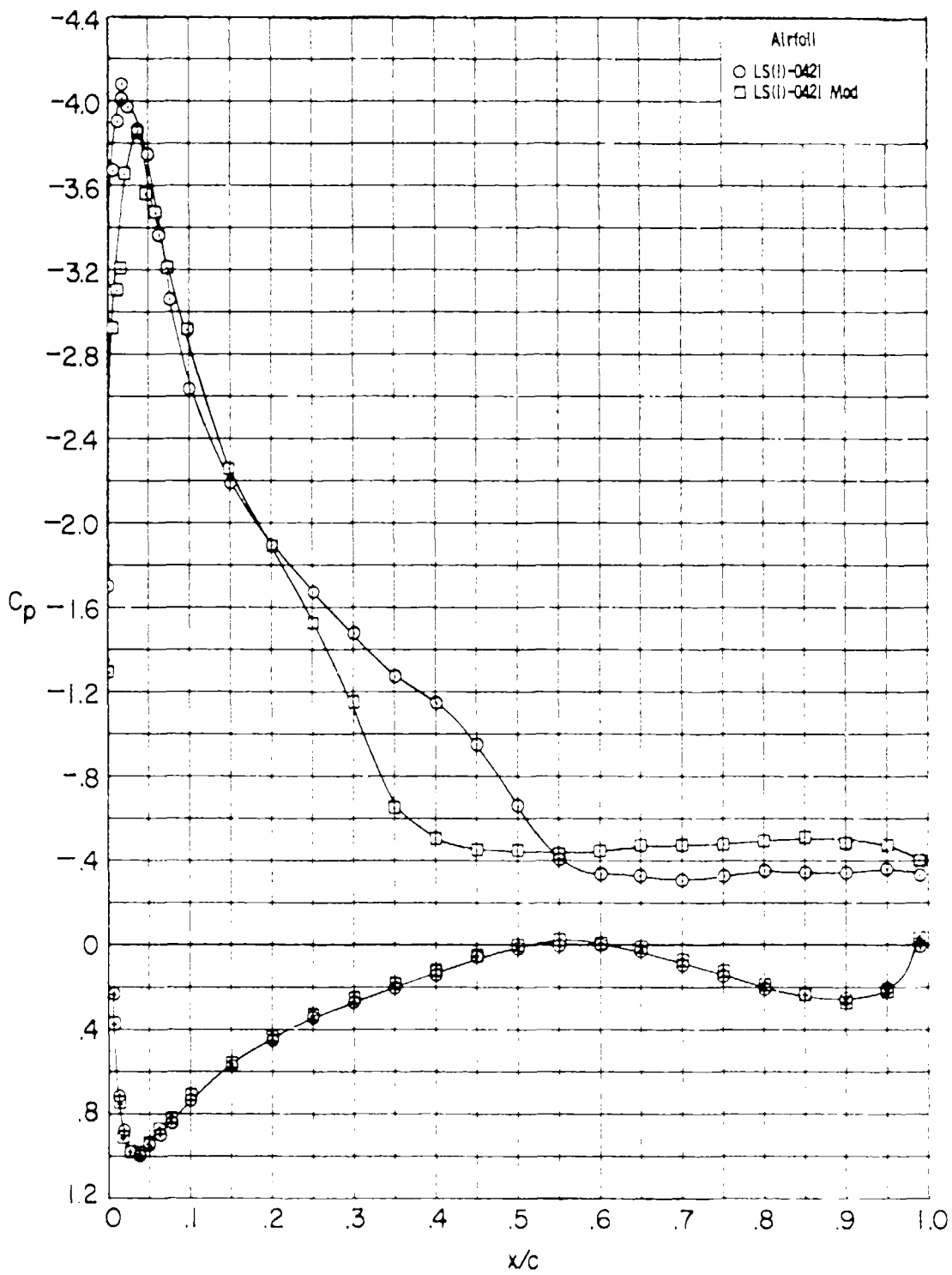
(d) $\alpha \approx 14°$; $R = 4.0 \times 10^6$.

Figure 12.- Continued.

(e) $\alpha \approx 0°$; $R = 9.0 \times 10^6$.

Figure 12.— Continued.

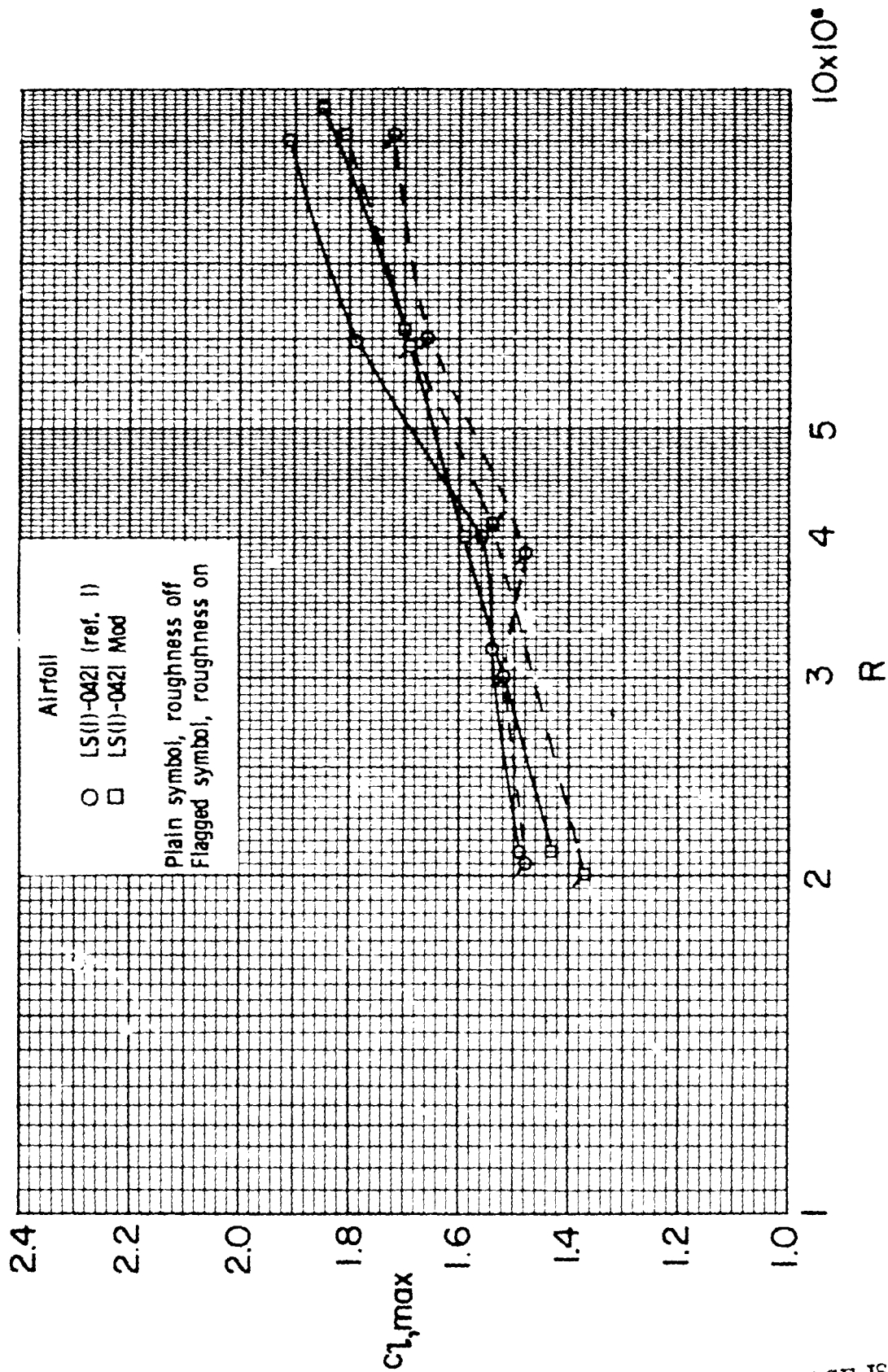(f) $\alpha \approx 4°$; $R = 9.0 \times 10^6$.

Figure 12.- Concluded.

41

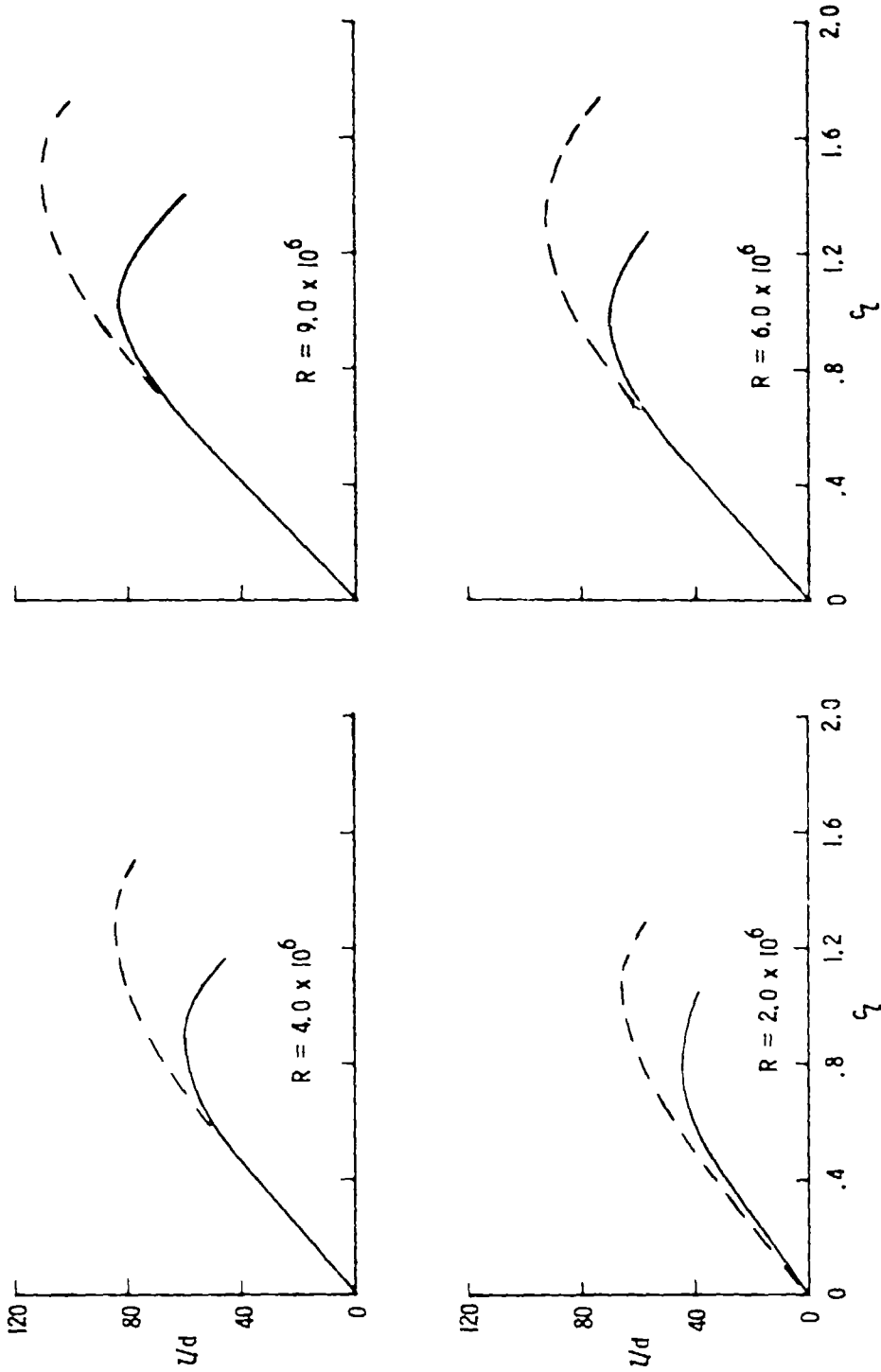Figure 13.- Variation of maximum lift coefficient with Reynolds number for LS(1)-0421 and LS(1)-0421 modified airfoils. M = 0.15.

Figure 14.- Variation of lift-drag ratio with lift coefficient for LS(1)-0421 and LS(1)-0421 modified airfoils. M = 0.15; roughness on.

43